Aus dem

Institut für Chirurgische Forschung im Walter-Brendel-Zentrum für Experimentelle Medizin

Institut der Ludwig-Maximilians-Universität München

Retinoic acid modulation guides human-induced pluripotent stem cell differentiation towards left or right ventricle-like cardiomyocytes

Dissertation

zum Erwerb des Doktorgrades der Medizin

an der Medizinischen Fakultät der

Ludwig-Maximilians-Universität zu München

vorgelegt von

Hengliang Zhang

aus

Luoyang, China

Jahr

2024

Mit Genehmigung der Medizinischen Fakultät der
Ludwig-Maximilians-Universität München

Erstes Gutachten:	Prof. Dr. Daphne Merkus
Zweites Gutachten:	Priv. Doz. Dr. Sebastian Clauß
Drittes Gutachten:	Prof. Dr. Robert Dalla Pozza

Promovierter Mitbetreuer:	Prof. Dr. Andreas Dendorfer
Dekan:	Prof. Dr. med. Thomas Gudermann

Tag der mündlichen Prüfung: 19.06.2024

Table of content

Zusammenfassung (Deutsch):

Hintergrund: Kardiomyozyten (Cardiomyocytes, CMs), die aus humanen induzierten pluripotenten Stammzellen (human induced pluripotent stem cells, hiPSCs) nach herkömmlichen Methoden abgeleitet werden, bestehen aus einer Mischung von Vorhofzellen, Kammerzellen und vielen anderen nicht-kardiomyozytären Zellen.

Ziel: Modulation mit spezifischen Konzentrationen von Retinsäure (Retinoic acid, RA), um die Differenzierung von hiPSC in Richtung links- und rechtsventrikulärer CM-Phänotypen zu fördern.

Methoden: hiPSCs wurden durch Reprogrammierung von Hautfibroblasten gewonnen. Unterschiedliche Konzentrationen (Kontrollgruppe ohne RA, LRA-Gruppe mit 0,05 μM und HRA-Gruppe mit 0,1 μM) von RA wurden während des dritten bis sechsten Tages des Differenzierungsprozesses verabreicht. Künstliche Herzgewebe (Engineered heart tissues, EHTs) wurden durch die Zusammenstellung von aus hiPSC abgeleiteten CMs (hiPSC-CM) in einer niedrigkollagenen Hydrogelmatrix erzeugt. Die Reifung und das Wachstum der EHTs wurden in einem maßgeschneiderten biomimetischen Gewebekultursystem induziert, das kontinuierliche elektrische Stimulation, Medium-Agitation und Dehnung bietet. Die Funktion der CMs und EHTs wurde unter verschiedenen Bedingungen analysiert. Schließlich wurden RNA-Extraktion und Gewebe-Fixierung an CMs und EHTs für RT-qPCR und Immunfluoreszenz-Färbungsanalyse durchgeführt. Die RNA-Sequenzierung wurde an EHTs durchgeführt, um zu untersuchen, wie RA die Expression von Genen moduliert, die an der Herzstruktur und -funktion beteiligt sind.

Ergebnisse: In der HRA-Gruppe zeigten hiPSC-CMs erstmals eine schlagende Aktivität und wiesen die höchste Expression von Reifegenen wie MYH7 und cTnT auf. Die Expression von TBX5, NKX2.5 und CORIN, die Marker-Gene für linksventrikuläre CMs sind, war ebenfalls in der HRA-Gruppe am höchsten. Der Transkriptionsfaktor MEF2C, der mit RA und ventrikulären Entwicklungs-Genen in Verbindung steht, NPPA und MYH6, wurde in der HRA-Gruppe stark exprimiert, während GATA4 in der HRA-Gruppe weniger exprimiert wurde. In Bezug auf EHT zeigte die HRA-Gruppe die höchste Kontraktionskraft, die niedrigste Schlagfrequenz und die höchste Empfindlichkeit gegenüber Hypoxie und Isoprenalin, was bedeutet, dass sie funktionell dem linken Ventrikel ähnlicher war. Die Expression von TBX5 und NKX2.5 war in der HRA-Gruppe von EHT am höchsten, während die Expression von TBX20 und ISL1 in der Kontrollgruppe am höchsten war. Wenn die elektrische Stimulationsfrequenz von EHT in der HRA-Gruppe erhöht wurde, stieg entsprechend die Kontraktionskraft. Die gesteigerte Kontraktilität von EHT in der HRA-Gruppe kann auf die Förderung der extrazellulären Matrixstärke durch RA zurückgeführt werden.

Fazit: Durch Eingriffe in den Differenzierungsprozess von hiPSCs mit einer spezifischen Konzentration von RA zu einem bestimmten Zeitpunkt konnten wir erfolgreich CMs und EHTs mit einem Phänotyp erzeugen, der dem des linken oder rechten Ventrikels ähnelt. Unsere Forschung ebnet den Weg für zukünftige Studien zur In-vitro-Funktion des linken oder rechten Ventrikels, zur personalisierten Arzneimitteltestung und zur Präzisionsmedizin.

Schlüsselwörter: Retinsäure, hiPSC, Kardiomyozyt, Künstliches Herzzgewebe, Linker Ventrikel.

Abstract (English):

Background: Cardiomyocytes (CMs) derived from human induced pluripotent stem cells (hiPSCs) by traditional methods are a mix of atrial and ventricular CMs and many other non-cardiomyocytes. Retinoic acid (RA) plays an important role in regulating the spatiotemporal development of the embryonic heart and high concentrations of RA have been shown to steer differentiation towards atrial CMs, whereas lower concentrations of RA promote a more ventricular-like CM profile.

Aim: Create engineered heart tissue (EHT) with left and right ventricular phenotypes from hiPSCs by intervening with specific concentrations of retinoic acid (RA) during hiPSC differentiation towards CM.

Methods: hiPSC were derived by reprogramming skin fibroblasts and erythroid progenitors. Different concentrations of RA (Control group without RA, LRA group with 0.05 μM and HRA group with 0.1 μM) were administered during the third to sixth days of the differentiation process. Engineered heart tissues (EHTs) were generated by assembling CMs derived from hiPSC (hiPSC-CM) at high cell density in a low collagen hydrogel. The maturation and growth of EHTs were induced in a customized biomimetic tissue culture system, that provides continuous electrical stimulation, medium agitation and stretch. The function of CMs and EHTs was analyzed under different conditions. Finally, RNA extraction and tissue fixation were performed on CMs and EHTs for RT-qPCR and immunofluorescence staining analysis. RNA sequencing was conducted on EHTs to examine how RA affects signaling involved in the function and structure of EHT

Results: In the HRA group, hiPSC-CMs exhibited the first onset of beating and showed the highest expression of maturity genes MYH7 and cTnT. The expression of TBX5, NKX2.5 and CORIN, which are the marker genes for left ventricular CMs, was also the highest in the HRA group. The transcription factor MEF2C associated with RA, was highly expressed in the HRA group, while GATA4 was less expressed in the HRA group. In terms of EHT, the HRA group displayed the highest contraction force, the lowest beating frequency, and the highest sensitivity to hypoxia and isoprenaline, which means it was more functionally similar to the left ventricle. The expression of TBX5 and NKX2.5 was found to be the highest expression in the HRA group of EHT, while expression of TBX20 and ISL1 was found to be the highest expression in control group. When the electrical stimulation frequency of EHT in the HRA group was raised, it

correspondingly increased its contractile force. The heightened contractility of EHT within the HRA group can be attributed to the promotion of augmented extracellular matrix strength by RA.

Conclusion: By interfering with the differentiation process of hiPSC with a specific concentration of RA at a specific time, we were able to successfully induce CMs and EHT with a phenotype similar to that of the left ventricle or right ventricle. Our research paves the way for future studies on *in vitro* left ventricular or right ventricular function, personalized drug screening, and precision medicine.

Key words: Retinoic acid, hiPSC, Cardiomyocyte, Engineered heart tissue, Left ventricle.

List of figures

List of tables

List of abbreviations

BMCC	Biomimetic cultivation chamber
BMP	Bone morphogenetic protein
CM	Cardiomyocyte
CORIN	Corin, serine peptidase
CPC	Cardiac progenitor cell
DMEM	Dulbecco's Modified Eagle Medium
DMSO	Dimethyl sulfoxide
E8	Essential 8
EDTA	Ethylenediaminetetraacetic acid
EHT	Engineer heart tissue
FGF	Fibroblast growth factor
FGF-2	Fibroblast growth factor 2
FHF	First heart field
GAPDH	Glyceraldehyde-3-phosphate dehydrogenase
GATA4	GATA binding protein 4
HAND1	Heart and neural crest derivatives expressed 1
hESC	Human embryonic stem cell
hiPSC	Human induced pluripotent stem cells
hiPSC-CM	Cardiomyocyte derived from human induced pluripotent stem cell
HRA	High concentration retinoic acid
IGF-1	Insulin-like growth factor 1
IMDM	Iscove's Modified Dulbecco's Medium
ISL1	ISL LIM homeobox 1
LRA	Low concentration retinoic acid
MEF2C	Myocyte enhancer factor 2C

MYH6	Myosin heavy chain 6
MYH7	Myosin heavy chain 7
MYL2	Myosin light chain 2
MYL7	Myosin light chain 7
NKX2.5	NK2 homeobox 5
NPPA	Natriuretic peptide A
NPPB	Natriuretic peptide B
NR2F2	Nuclear receptor subfamily 2 group F member 2
PBS	Phosphate buffer saline
PCR	Polymerase chain reaction
PFA	Paraformaldehyde
PPI	Protein-protein interaction
RA	Retinoic acid
RAR	RA receptors
RARE	Retinoic acid response elements
RIN	RNA Integrity number
SEM	Standard error of the mean
SHF	Second heart field
TBX20	T-box transcription factor 20
TBX5	T-box transcription factor 5
TGF-ß1	Transforming growth factor-β1 transcription factor (TF)
t-SNE	t-distributed stochastic neighbor embedding
VEGF165	Vascular endothelial growth factor isoform 165
WGA	Wheat germ agglutinin
min	Minute
3D	3 Dimension
N	Number
mM	Millimol/Liter
µM	Micromol/Liter

nM	Nanomol/Liter
ml	Milliliter
µl	Microliter
mg	Milligram
µg	Microgram
mm	Millimeter
µm	Micrometer
mN	MilliNewton
µN	MicroNewton
nN	NanoNewton
Hz	Hertz

1. Introduction

1.1 Human induced pluripotent stem cell

Human induced pluripotent stem cells (hiPSCs) represent a distinct category of stem cells generated through the reprogramming of adult somatic cells, such as skin or blood cells, into a pluripotent state(1). This reprogramming process involves the introduction of specific genetic factors into adult cells, triggering their transformation into a state akin to embryonic stem cells. The identification of hiPSCs marked a significant milestone in the realm of regenerative medicine(2). Preceding this breakthrough, human embryonic stem cells (hESCs), derived from early-stage embryos, served as the primary reservoir of pluripotent stem cells for research and therapeutic applications(3). However, the utilization of hESCs gave rise to ethical concerns and became subject to regulatory restrictions in numerous nations.

The derivation of hiPSCs has effectively circumvented ethical and legal barriers by directly originating from adult cells. This breakthrough has significantly broadened horizons for investigating human development, disease modeling, drug screening, and personalized medicine(4-6). Through the reprogramming of cells obtained from patients with genetic disorders or diseases, scientists can establish hiPSC lines harboring identical genetic mutations, enabling the exploration of the fundamental mechanisms underlying these conditions and the development of tailored therapies(7). hiPSCs exhibit several pivotal characteristics that render them invaluable for both research and clinical applications(8). They possess self-renewal capabilities, enabling division and the generation of additional hiPSCs. Moreover, their pluripotency allows differentiation into cells representing all three germ layers: ectoderm, endoderm, and mesoderm. Simultaneously, hiPSCs demonstrate adaptability in producing diverse cell types applicable within the human body, including neurons, cardiomyocytes, and hepatocytes. Cardiomyocytes (CMs) derived from human induced pluripotent stem cells (hiPSC-CM) exhibit a differentiation principle akin to that of CMs derived from embryonic stem cells. The ethical advantages and superior differentiation efficiency associated with hiPSC-CM have fostered a wide array of promising applications.

1.2 Differentiation processes in the embryonic heart and hiPSC-CM

Biologists have been fascinated by the molecular regulation of heart development for more than a century. Scientists in the field of cardiac developmental biology have dedicated substantial research efforts to unraveling the intricate mechanisms governing heart formation. They are driven by a desire to enhance our understanding of congenital heart disease and explore regenerative medicine prospects. Researchers increasingly focus on the interaction between signaling molecules and transcription factor networks that guide the commitment of CM lineages and the specification of cardiac chambers. The successful induction of hiPSCs through gene modification techniques has positioned them as a viable alternative to embryonic stem cells. The process of differentiating hiPSCs into various cardiac cells closely mirrors the molecular regulatory mechanisms active during embryonic development leading to a mature heart. The ability to precisely control the differentiation of hiPSCs into distinct subtypes of cardiomyocytes is crucial for generating *in vitro* models for specific cardiovascular diseases and advancing innovative treatments(9). Consequently, the investigation of molecular mechanisms and regulatory factors during embryonic heart development forms the foundation for the precise differentiation of hiPSC-derived cardiomyocytes (hiPSC-CM).

Cardiac development originates from bilateral cardiac fields established during gastrulation(10). The antero-lateral plate mesoderm is initially molded as cardiac field precursors migrate anteriorly and laterally from the primitive streak, followed by rapid convergence toward the midline(11). The linear heart tube forms through subsequent fusion at the midline, facilitated by the closure of the foregut(12). In late gastrulation, the cardiac crescent emerges, consisting of cardiac progenitors derived from both the first heart field (FHF) and the second heart field (SHF) (Figure 1)(13). As cells mature and develop, the FHF forms a linear heart tube, predominantly contributing to the left ventricle (LV) and a portion of the atria. Conversely, posterior SHF cells give rise to the atria and the inflow tract, whereas anterior SHF cells contribute to the right ventricle (RV) and the outflow tract(13, 14). The linear heart tube undergoes extension and rightward looping to position the atria cranially in relation to the ventricles. Several remodeling events are necessary to facilitate septation, valve development, and the formation of a four-chambered heart(15). The heart is now fully functional and responsible for pumping blood from the venous pole to the arterial pole(16).

In this stage, precise regulation of molecular signaling pathways during embryonic development is essential for the heart's ability to generate blood flow(16, 17). Bone morphogenetic proteins (BMPs) (18, 19), T-box transcription factors, and non-canonical Wnt/JNK(20) are among the pro-cardiogenic factors expressed in FHF and SHF. Precisely regulating the spatial and temporal distribution of transcription factors in this intricate process is essential for ensuring the heart's correct morphological and functional differentiation(14).

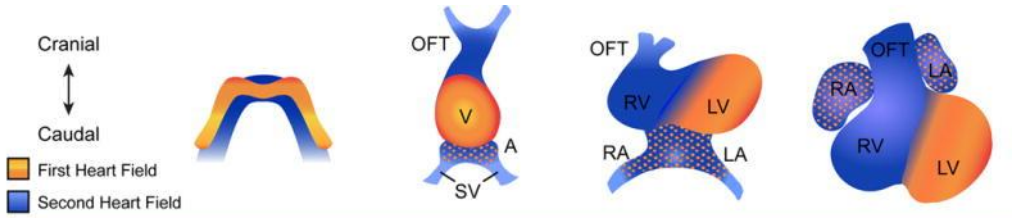

Stage	Cardiac Crescent	Linear Heart Tube	Looping Heart	Chamber Specialization/ Septation
Mouse Embryo Stage	E7.5	E8.0	E9-12	E10+
Human Embryo Stage	Day 15	Day 20	Day 28-30	Day 32+
Key Regulators	GATA4 NKX2.5 MESP1/2 ISL1 BAF60C MEF2C	GATA4 NKX2.5 TBX5 TBX20 MEF2C	GATA4 NKX2.5 TBX5 MEF2C HAND1/2	GATA4 NKX2.5 TBX5 PITX2 TBX1

Figure 1. Overview of heart development(14).

Transcriptional regulators for each stage of heart development are listed. The colour orange represents the FHF and its derivatives, while blue represents the SHF and its derivatives.

1.3 The application of EHT

Engineered heart tissue (EHT) represents a laboratory-fabricated three-dimensional arrangement of cardiac cells meticulously designed to closely imitate the structure and functionality of native cardiac tissue(21). EHTs are typically produced through a synergistic combination of various cardiac cell types, such as cardiomyocytes, fibroblasts, or endothelial cells, along with biomaterials and advanced tissue engineering methodologies(22). The development of EHTs is now widely acknowledged as a promising approach in the fields of regenerative medicine and cardiovascular research(22). These tissue constructs are intricately engineered to faithfully replicate both the architectural complexities and physiological characteristics of the heart. This enables scientists to explore the nuances of cardiac biology, simulate

heart diseases, and investigate potential therapeutic interventions for cardiac conditions(23).

EHTs exhibit several vital characteristics. They display spontaneous contractility, emulating the functional behavior of native cardiac tissue. EHTs demonstrate electrical activity, responsiveness to external stimuli, and the presence of crucial molecular markers and structural features similar to those found in native heart tissue. Therefore, EHTs offer a wide array of applications in both research and clinical domains, serving as invaluable models for investigating cardiac development, unraveling disease mechanisms, facilitating drug screening, and conducting toxicology testing(24). EHTs can also be utilized to evaluate the effectiveness and safety of potential cardiac therapies or serve as a foundation for personalized medicine strategies(25), which could potentially substitute or repair damaged or afflicted cardiac tissue, providing an alternative to traditional transplantation methods. The use of a patient's own cells might mitigate the risk of rejection, making EHTs an attractive choice for cardiac regeneration.

However, despite significant progress in EHT research, substantial challenges persist(26, 27). Ongoing areas of research and development include achieving complete maturation of cardiac cells within the construct, ensuring scalability for clinical applications, and integrating vascularization to supply essential nutrients and oxygen to the tissue. In a broader context, EHTs represent a significant advancement in cardiac research and regenerative medicine, offering a promising avenue for understanding cardiac biology, innovating new therapies, and potentially addressing heart-related diseases.

1.4 Disadvantages of EHT and CM derived from hiPSC

The primary challenge associated with CM and EHT derived from hiPSC is their inability to fully replicate the heart's genetic, protein, and phenotypic complexity. The existing differentiation scheme for hiPSCs yields cardiomyocytes displaying immature phenotypes reminiscent of fetal developmental stages(28, 29). Consequently, researchers have increasingly shifted their focus, seeking alternative perspectives to enhance hiPSC-CM maturity. Notably, Liu et al. discovered that the PGC-1α activator ZLN005 promotes mitochondrial biology and energy metabolism maturation, augments structural development, specifically sarcomere length, and elevates the expression of CX43. This activation also enhances electrical activity, Ca^{2+} handling, and

electrophysiological features while fostering the maturation of hiPSC-CMs(30). In parallel, Miki et al. demonstrated that ERRγ agonists enhance hiPSC-CMs by increasing cell volume, sarcomere length, transverse tubule presence, and metabolic function. These enhancements correlate with the attributes of mature neonatal CMs and have implications for disease modeling and regenerative medicine(31). The combination of hiPSC-derived CMs, cardiac fibroblasts (CF), and cardiac endothelial cells fosters the maturation of scaffold-free three-dimensional microstructures(32). Furthermore, employing EHTs to subject developing cardiomyocytes to the electromechanical forces inherent in the heart has demonstrated efficacy in surmounting developmental impediments and promoting further maturation(33-35). These collective investigations lay a solid foundation for the application of hiPSC-CM and EHT in research and clinical contexts.

Another challenge is the current inability to precisely control the differentiation of hiPSC into specific myocardial tissue phenotypes. EHT and CMs induced from hiPSCs using traditional methods represent a heterogeneous population comprising both atrial and ventricular cells (Figure 2)(36, 37). Although, earlier studies have effectively accomplished the differentiation of hiPSC-CM into distinct atrial or ventricular phenotypes(38, 39). Numerous studies have achieved successful differentiation of hiPSCs into CMs exhibiting a sinoatrial phenotype(40, 41). The differentiation technology for non-CMs, such as the epicardium, has reached a high level of advantage(42, 43). Nevertheless, no prior research has achieved the successful differentiation of hiPSC-CM into EHT with specific phenotypes corresponding to either the left ventricle (LV) or the right ventricle (RV).

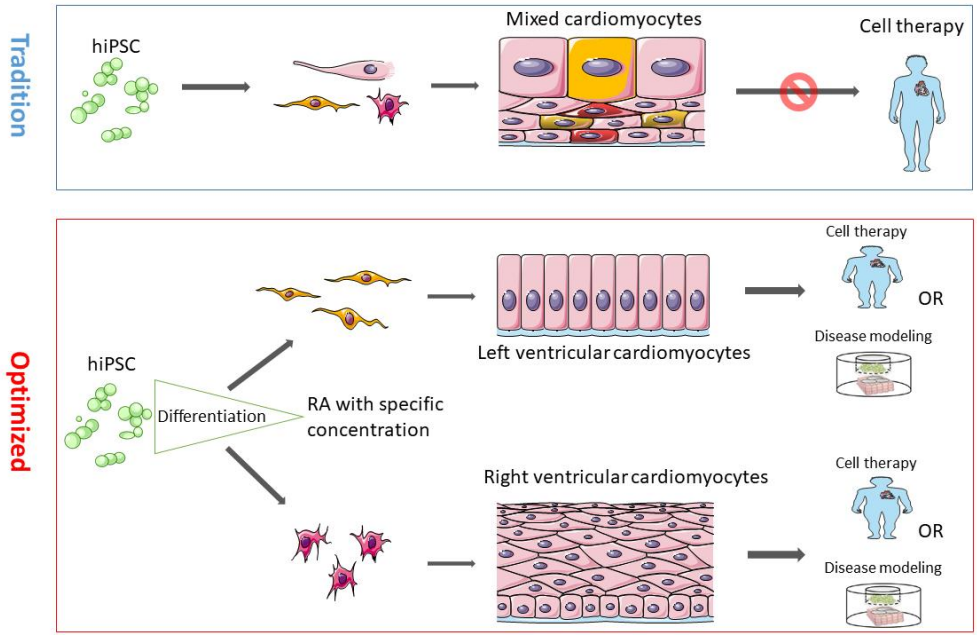

Figure 2. Clinical significance of left ventricular or right ventricular CMs cultured *in vitro* and schematic representation of our differentiation and maturation protocol.

The upper panel shows the traditional method of inducing differentiation. The lower panel shows our optimized method.

1.5 The effect of retinoic acid on hiPSC

Retinoic acid (RA) signaling plays a pivotal role in embryonic development, as it is essential for organizing the trunk and facilitating organogenesis in diverse tissues derived from all three germ layers(44, 45). In addition to being one of the ingredients regulating embryonic development, RA also regulates cardiac development and affects the differentiation of hiPSC-CM into different subtypes, with the direction of differentiation being time- and concentration-dependent(46). Previous research has demonstrated that RA concentrations ranging from 1 μM to 5 μM appear to promote hiPSC-CM or heart embryonic differentiation toward atrial CMs(38, 39, 46), whereas a concentration of 0.05 μM appears to promote differentiation towards left ventricular CMs(47). Other studies found that RA mainly induces epicardial cells at 1 μM to 4 μM(42), while RA intervenes in the mesoderm between 0.5 and 1.0 mM to enhance the fraction of atrial cardiomyocytes(39, 48) (Figure 3).

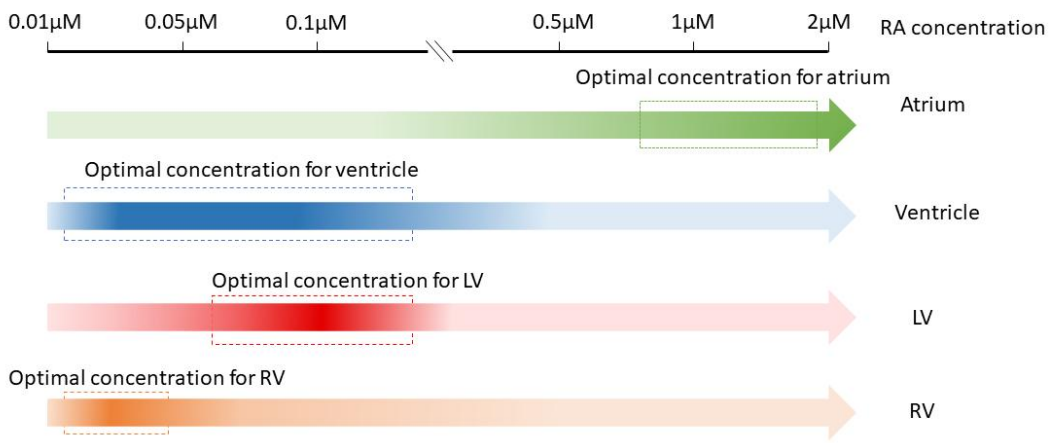

Figure 3. Retinoic acid (RA) regulates the differentiation direction of CMs in a concentration dependent manner.

Beyond the RA concentration, the timing of RA intervention is crucial. Recent *in vivo* and *in vitro* findings show that applying RA intervention at different stages of embryonic stem cell differentiation yields diverse functional traits and phenotypes in resulting cardiomyocytes(49). Previous research has shown that applying RA intervention during the later stages of mesoderm development (days 2-4) supports the differentiation of embryonic stem cells into cardiomyocytes (CMs)(37, 50). Particularly, treatment with RA between days 15 and 20 enhances cardiomyocyte area, sarcomere length, multinucleation, and mitochondrial copy number(51). While the timing of RA intervention differs across studies, there is a consensus indicating that the RA pathway intervention significantly influences stem cell differentiation around the 4th day. In our research, we relied on recent *in vivo* and *in vitro* findings(37, 49, 50, 52) to establish the best timing and duration for RA intervention. Subsequently, we hypothesized that the mesoderm induction stage (days 3-6) with a lower RA dosage is critical for ventricular chamber specification.

Numerous studies have endeavoured to uncover the regulatory relationships among transcription factors associated with heart development. RA has been shown to operate upstream of the transcription factor TBX5, indirectly modulating its expression(53, 54). During heart development, the transcription factors TBX5, NKX2.5, and GATA4 interact with each other to regulate signal transduction pathways(55-57). GATA4 activates the expression of NKX2.5, and both GATA4 and NKX2.5 activate the expression of TBX5(58-60). Additionally, the proteins NKX2.5 and MEF2C have been linked to ventricular CM differentiation(61-63). TBX5 alone or in combination with

GATA4, NKX2.5 and MEF2C regulates the expression of multiple target genes that are critical to the structure and function of the heart, including MYH6, MYH7 and NPPA(64, 65). Hence, RA concentrations may govern gene and protein expression crucially involved in heart morphogenesis (Figure 4) and modulating RA concentrations may provide a tool to direct CM-differentiation towards LV and RV phenotypes.

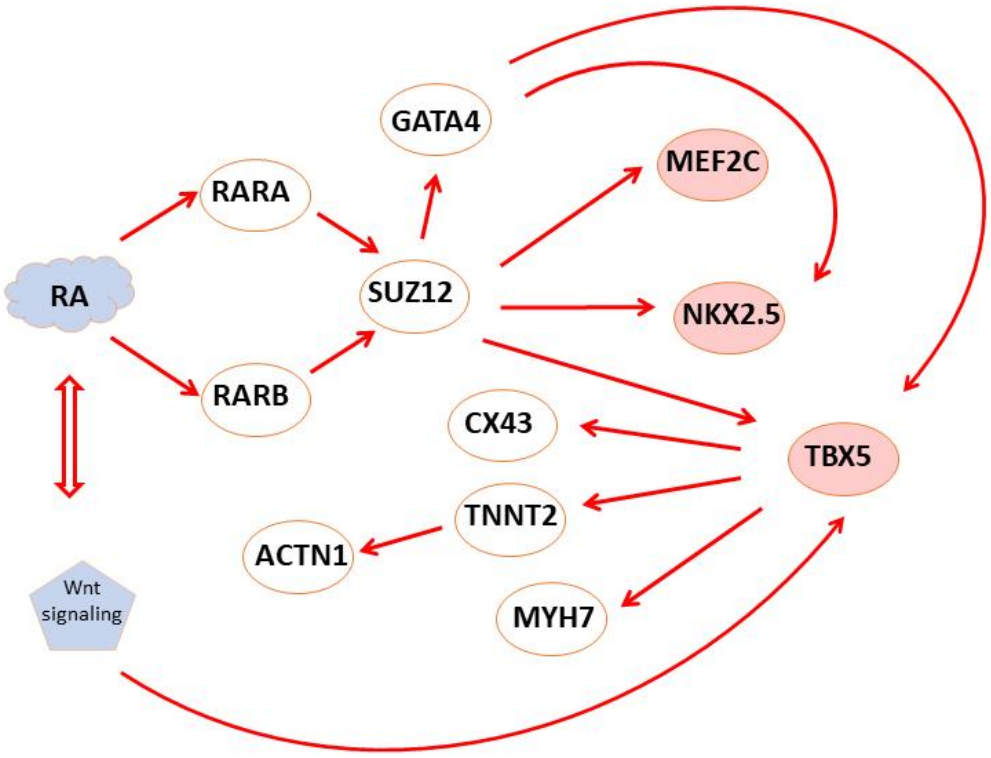

Figure 4. RA regulates hiPSC-CM differentiation direction through transcription factors.

1.6 Research objective

Given the significant impact of RA on the differentiation of embryonic stem cells and hiPSC into CMs, our research aims to explore a new method of left and right ventricular CM and subsequent EHT generation while optimizing concentration and timing of RA intervention during hiPSC differentiation. Specifically, the first aim of our study was to investigate whether specific concentrations of RA can guide the hiPSCs differentiation towards LV and RV phenotypes. To achieve the goal, we intervened in the differentiation process of hiPSC-CM with different concentrations of RA during the 3rd to 6th days, according to the previous study(39, 47). To verify whether the

differentiated hiPSC-CM were LV and/or RV-like, we derived LV and RV specific marker genes from single-cell RNA sequencing data available in literature, and subsequently analyzed the function, maturity and specificity of ventricular marker genes of CMs. The second aim of our study was to investigate whether the LV and RV phenotypes of the iPSC-derived CMs were preserved in EHTs, which more closely mimic functional myocardial tissue. Consequently, the contractile force of EHTs was examined and compared, alongside its responses to hypoxia, β-receptor agonists, and electrical stimulation (Figure 5).

Our research aims to investigate the following questions:

1. What is the optimal RA concentration for promoting hiPSC differentiation into CMs with left or right ventricular phenotypes?

2. What are the effects of different concentrations of RA on EHT function and gene phenotype?

3. What potential mechanisms underlie RA's influence on ventricular differentiation?

4. Does RA have an effect on the extracellular matrix of EHTs?

5. Whether high-frequency electrical stimulation impact the contractile function of EHTs?

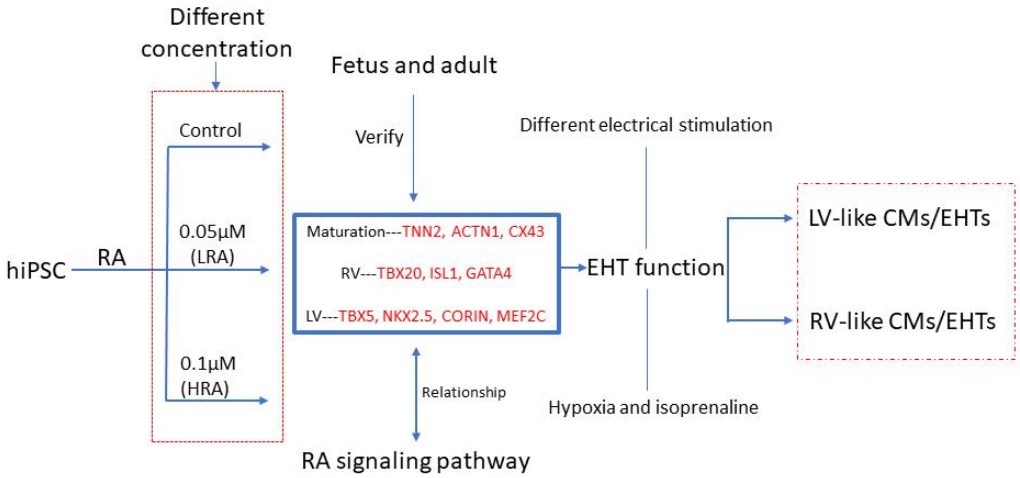

Figure 5. Schematic presentation of this study.

Gene names with a red colour represent marker genes or/and transcription factor (TF) genes. hiPSC: human induced pluripotent stem cell. RA: Retinoic acid. LRA, low concentration RA-- 0.05 μM. HRA, high concentration RA-- 0.1 μM. LV: Left ventricle. RV: Right ventricle. EHT: Engineered heart tissue. CM: Cardiomyocyte.

2. Material and Methods

2.1 Material

2.1.1 General Laboratory Devices and Equipments

Cell culture incubator	Thermo Fisher Scientific, USA
Centrifuge, Heraeus Megafuge 40R	
Cell culture incubator, BINDER CB160	BINDER, Germany
Centrifuge, Rotina 35R	Hettich, Germany
Shaking water bath, SWB25	Thermo Haake, USA
Shaking air bath, UNIMAX 1010	Heidolph, Germany
Digital Vortex Mixer	VWR, USA
Countess Cell Counter	Life Technologies, USA
+4°C fridge	LIEBHERR, Germany
-20°C fridge	Privileg, Germany
-80°C fridge	Heraeus Holding GmbH, Germany
Thermo-Shaker, PCMT	Grant Instruments, UK
Inverted microscope	Zeiss, Germany
StepOnePlus Real-Time PCR System	Applied Biosystems, USA
Simplinano Spectrophotometer	Biochrom, USA
TriM Scope I -Photon Microscope	LaVision Biotech, Germany

Carl Zeiss, Axio Zoom.V16	Carl Zeiss, Germany
Illumina HighSeq-2000 platform	Illumina, USA

2.1.2 hiPSC cell line

	Clone 1	Clone 2
Cell line name	MRIi-004-A	EMC238i
Parental cell type	Skin Fibroblast	Erythroid Progenitors
Species of origin	Homo sapiens	Homo sapiens
Category	Induced pluripotent stem cell	Induced pluripotent stem cell
Diagnosis	Health	Health
Matrix	Geltrex	Geltrex

2.1.3 Cell culture medium and other supplements

IMDM	Gibco, USA
DMEM	Gibco, USA
DMEM X10	Gibco, USA
DMEM/F-12	Gibco, USA
Essential 8™ Medium	Gibco, USA
EHT culture medium	Custom made
EB6 medium	Custom made
B27 minus Insulin	Gibco, US

MEM non-essential amino acids	Gibco, US
Penicillin G sodium salt, P3032	Sigma Aldrich, USA
Streptomycin sulfate salt, S9137	Sigma Aldrich, USA
Penicillin-Streptomycin (10,000 U/mL)	Gibco, US
Dexamethasone	Sigma Aldrich, USA
FGF-2, fibroblast growth factor-2	PEPROTECH, USA
IGF-1, insulin-like growth factor 1	PEPROTECH, USA
TGF-β1, transforming growth factor-β1	PEPROTECH, USA
VEGF165, vascular endothelial growth factor 165	PEPROTECH, USA
FBS Premium South America	PAN ™ Biotech, USA
beta-mercaptoethanol	Sigma-Aldrich, USA
3,3`,5-triiodo-L-thyronine	Sigma-Aldrich, USA

2.1.4 Chemical reagents

EDTA Versene solution	Gibco, USA
TrypLE Select Enzyme	Gibco, USA
Collagenase II	Sigma-Aldrich, USA
Bovine collagen I	Gibco, USA
Geltrex®, LDEV-Free	Gibco, USA
RevitaCell supplement	Gibco, USA

Retinoic acid	Sigma-Aldrich, USA
DPBS	Gibco, USA
4% paraformaldehyde	Sigma-Aldrich, USA
1% Triton X-100	Thermo Fisher Scientific, USA
Fetal bovine serum	Gibco,USA
Isoproterenol	Sigma-Aldrich, USA
HEPES-buffered Earle' s-salt solution	Sigma-Aldrich, USA
30% Sucrose solution	Sigma-Aldrich, USA
7.5% gelatin	Sigma-Aldrich, USA
Isopentane	Sigma-Aldrich, USA
Glycerol solution	Sigma-Aldrich, USA
Blocking solution (3% bovine serum albumin in PBS)	Custom made
DAPI, 2 µmol/L	Invitrogen, USA
NaOH	Sigma-Aldrich, USA
MatriGel	Dow Corning, USA

2.1.5 Commercial kits

Essential 8™ Medium Kit	Gibco, USA
PSC Cardiomyocyte Differentiation Kit	Thermo Fisher Scientific, USA

RNeasy Mini Kit	Qiagen, Netherlands
QuantiTect ReverseTranscription Kit	Qiagen, Netherlands
SENSE Total RNA-Seq Library Prep Kit	Lexogen, Austria

2.1.6 Antibodies

First Antibody	
Monoclonal anti-α-actinin, sarcomeric, 1:100, GR3356520-3	Abcam, UK
Second Antibody	
Alexa Fluor 594 anti-Rabbit IgG, 1:100, GR3323881-1,	Abcam, UK

2.1.7 Software

GraphPad Prism 7	California, USA
StepOne Software	Applied Biosystems Corporation, USA
ImageJ	National Institute of Health, USA
PowerLab 4/20; LabChart Reader	ADInstruments, Dunedin, New Zealand
Zeiss ZEN Imaging Software	Zeiss, Germany
Illumina software BaseCaller	Illumina, USA
R software version 4.3.1	University of Auckland, New Zealand

2.2 Methods

2.2.1 Analysis of the fetal heart single-cell RNA sequencing dataset

The single-cell RNA sequencing dataset (GSE106118) was acquired from Gene Expression Omnibus (GEO) (https://www.ncbi.nlm.nih.gov/geo/)(66). This dataset included human fetal ventricular specimens obtained from aborted fetuses aged 5 to 24 weeks with appropriate informed consent and ethics approval. The study elucidated the systematic mapping of the transcriptomic landscape of the human fetal heart. But the authors didn't compare the transcriptomic specificity of LV and RV. We analyzed the characteristics of the fetus's early development of the LV and RV in order to identify marker genes for our research. Genes having an adjusted p-value < 0.05 and a $|\log_2$ fold change$| > 2$ were deemed to be differentially expressed gene (DEG) when utilizing the FindMarkers tool in Seurat to analyze differential gene expression. The FindClusters function of the "Seurat" package was used to undertake cell-clustering analyses at the appropriate resolutions. The detected cell clusters were displayed using t-distributed stochastic neighbor embedding (t-SNE). The data were automatically annotated through HumanPrimaryCellAtlasData (https://rdrr.io/github/LTLA/celldex/man/HumanPrimaryCellAtlasData.html). In order to increase the accuracy of annotations, the annotation results were rechecked based on highly expressed genes, uniquely expressed genes, and reported canonical cellular markers.

2.2.2 Verify the marker gene

The marker genes for LV and RV were verified in human and swine heart tissue.

Human tissue:

Transmural slices of left and right ventricular myocardium measuring $2 \times 2\ cm^2$ were taken from failing hearts at the time of transplantation by the Clinic of Cardiac Surgery, Ludwig-Maximilians-University (LMU) Hospital, Munich, Germany. The patients gave informed consent for the scientific use of the explanted tissue, and the study was approved by the institutional ethics boards of the clinical and experimental study contributors, in accordance with the ethical standards of the 1964 Helsinki Declaration and its subsequent amendments. Upon retrieval, myocardial specimens were immediately placed in cold (4 °C) cardioplegic buffer (136 mM NaCl, 5.4 mM KCl, 1 mM $MgCl_2$, 0.33 mM NaH_2PO_4, 10 mM glucose, 0.9 mM $CaCl_2$, 30 mM 2,3-

butadione-2-monoxime, 5 mM HEPES, pH 7.4). Tissues were sectioned to 1 cm×2 cm×300 µm using a vibratome (Leica Biosystems). Slices were secured in biomimetic cultivation chambers (BMCC) according to fibre direction with tissue adhesive (histoacryl; B. Braun) and subjected to a physiological preload of 1 mN and stimulation at 1 Hz, as previously described(67). In an incubator, the BMCCs were secured on a rocker. Contractile force was measured continuously, and data were imported and analyzed using LabChart Reader software (AD Instruments, V8.1.14).

Swine tissues:

The left and right ventricular myocardial samples were obtained from swine undergoing experiments for various studies in our team(68). All animal experiments were approved by the *Regierung von Oberbayern* (ROB-55.2-2532.Vet_02-19-163) at the Institute of Surgical Research at the Walter-Brendel-Centre of Experimental Medicine, Munich, Germany and performed in accordance with the guidelines from Directive 2010/63/EU of the European Parliament on the protection of animals used for scientific purposes. Briefly, swine were sedated using a cocktail of ketamine (20 mg/kg Zoetis, Berlin, Germany) and azaperone (10 mg/kg, Elanco, Bad Homburg, Germany) and atropine (0.05 mg/kg, Braun Melsungen, Germany) im. Once sedated, midazolam (0.5 mg/kg), propofol (0.5 mg/kg/min) and sufentanil (10 µg kg^{-1} h^{-1}) were infused i.v to maintain anesthesia[30, 31]. Following intubation and hemodynamic measurements, the thorax was opened with a median sternotomy and the heart excised. Left and right ventricle were separated, weighed, cut into small pieces, immediately placed in liquid nitrogen and stored at -80 °C.

2.2.3 Cell culture and differentiation of hiPSC-CMs

Pluripotent stem cells were obtained by reprogramming somatic cells from two healthy human donors (induced two clones of hiPSC) according to the prescribed methods(69). Clone 1 was originally derived from skin fibroblasts, while clone 2 was derived from erythroid progenitors. The research project complied with the Declaration of Helsinki's guiding principles, and the study subjects gave written, informed permission. Our cultivation and differentiation process for hiPSC was mainly based on the methods summarized by our team previously(35). The hiPSCs were grown in matrix-coated dishes (Geltrex LDEV-Free, Gibco) with Essential 8 media (Gibco), which underwent daily replacement for maintenance. At 85% confluence, cells were divided and ethylenediaminetetraacetic acid (EDTA, Versene solution; Gibco) was used

to dissociate them. Chen and colleagues adapted a cutting-edge differentiation method for hiPSC-CMs that makes use of small molecules to promote differentiation(70). In brief, cardiac differentiation was triggered when the cells reached around 85% confluence by utilizing chemically defined elements for 24 hours (Cardiomyocyte differentiation medium A) and subsequently Cardiomyocyte differentiation medium B (PSC Cardiomyocyte Differentiation Kit; Gibco) for 48 hours. After 72 hours, differentiation of hiPSC-CMs was sustained for 12 days using cardiomyocyte maintenance medium (PSC Cardiomyocyte Differentiation Kit; Gibco), which was refreshed every other day. The role of cardiomyocyte differentiation medium A is to push hiPSCs toward mesodermal commitment via BMP/activin pathway activation and glycogen kinase 3 inhibition, while cardiomyocyte differentiation medium B induces cardiac mesoderm via Wnt inhibition. The function of cardiomyocyte medium maintenance is to mature cardiomyocytes. During the 3rd to 6th days of differentiation, different concentrations of RA (dissolved in DMSO) were introduced into cardiomyocyte maintenance medium (Figure 6). RA was added in two concentrations: 0.05 μM (LRA, Low concentration retinoic acid) and 0.1 μM (HRA, High concentration retinoic acid), while the control group received the same concentration of DMSO as the other two groups, without RA. hiPSC-CMs began to beat spontaneously starting on the 7th or 8th day of the differentiation protocol. Hence, we recorded the beating frequency of each well in each group from day 8 onwards.

On day 14, the contraction time and relaxation time of the hiPSC-CMs were measured, by analysis of videos (frame rate: 10 frames per second (fps)) of hiPSC-CMs beating under a microscope. The onset of contraction, the onset of relaxation, and the conclusion of relaxation, were marked at their respective time points, and the time difference between these points was calculated to ascertain the durations of contraction and relaxation. To ensure accuracy, two people independently analyzed the same sample at different times and the mean of the results was taken. On day 20, Isoprenaline was added in incremental concentrations to the wells, and changes in beating frequency as well as onset of contraction and relaxation were analyzed.

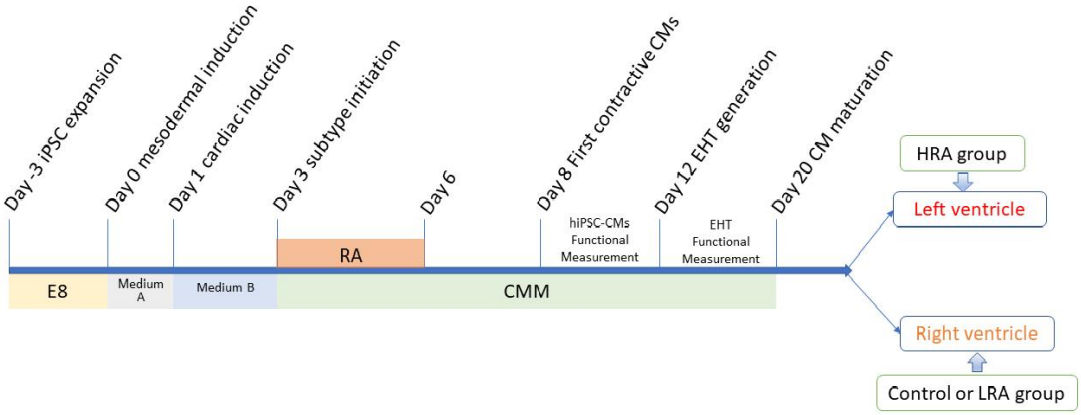

Figure 6. Workflow of the hiPSC-CM differentiation process.

From the 3rd to 6th days of differentiation, vehicle or RA was added to the control group (DMSO vehicle only), LRA (0.05 µM RA) and HRA (0.1 µM RA) group respectively.

2.2.4 Primary tissue assembly

Based on our team's prior methodology(35), collagenase II (1.5 mg/mL, Sigma-Aldrich) and TrypLE Select Enzyme (Gibco) were used to dissociate differentiated hiPSC-CMs for a total of 8 and 7 minutes, respectively. The cells were diluted with EB6 medium (Table 1), and then centrifuged at 390 g for 5 min. The cell pellet was suspended in medium with 0.55 mg/mL bovine collagen I (Gibco), 0.08 mg/mL Geltrex (LDEV-Free, Gibco), and 1% RevitaCell supplement, yielding a cell concentration of 1.1×10^5 cells/L (adapted from (71)). Following that, 55 µL of the cell-matrix combination was pipetted onto a 30 mm organotypic filter (PIC-MORG50, Merck Millipore) to form a disc approximately 8 mm in diameter and 2 mm thick. Following 30 minutes of solidification at 37 °C, 1 mL of EB 6 medium was introduced beneath the filter and refilled every other day for a total of 5 days in culture (Figure 7).

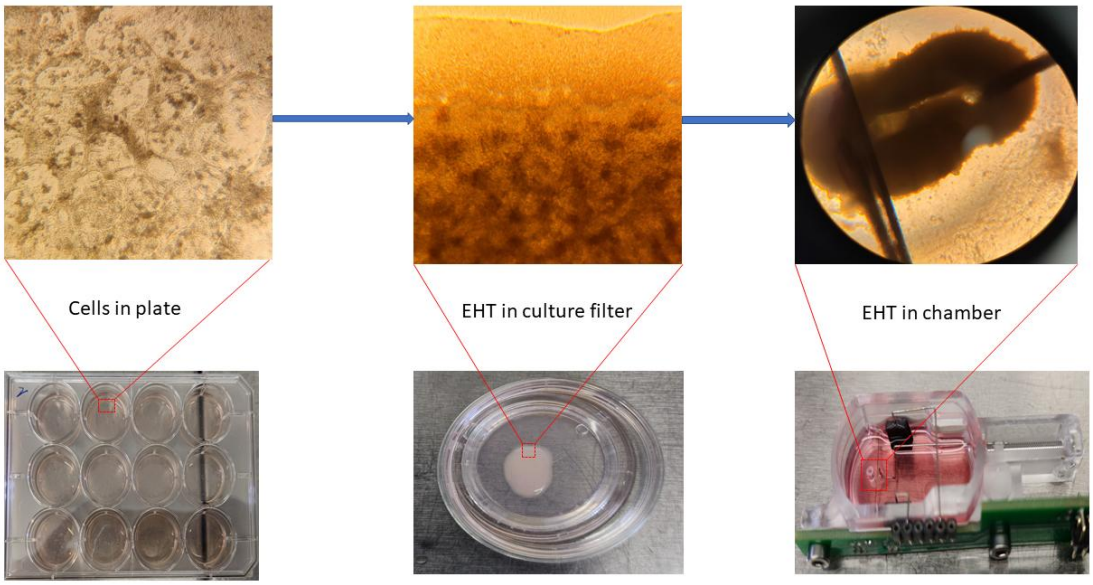

Figure 7. The process of making EHT and functional measurements.

Red boxes represent hiPSC-CMs (left), primary tissue (middle) and EHT (right), respectively.

Table 1 50 ml EB6 medium composition

Reagents	Stock	Volume
MEM Non-Essential Amino Acids (Gibco, 11140050)	100 X	1 ml
Penicillin/Streptomycin	100 X	5 ml
Fetal Bovine Serum (PAN Biotech)	-	3 mg
Beta-mercaptoethanol	20 mM	2.5 ml
DMEM/F-12 (Gibco, No. 11320033)	-	38.5 ml

2.2.5 Biomimetic culture of EHT

Our team developed a biomimetic cultivation technique for the long-term storage of adult human cardiac slices(67). We implemented the established parameters as the foundational conditions for EHT maturation because all biomimetic components of the cultivation device, such as precise preload, afterload, continuous bipolar stimulation, and medium agitation, has been deemed critical for the sustained performance of cultured human myocardium. According to Fischer et al. (67), biomimetic cultivation chambers (BMCCs) provide elastic attachment, length modification, electrical stimulation, and continuous force monitoring via magnetic position detection (Figure

8A). We used this system and implemented the optimized protocol for EHT maturation as detailed below(35).

The modified chambers used in this study were built with injection-molded polystyrene blanks (Proto Labs Feldkirchen, Germany). The chambers used a 0.16 mm diameter spring wire (stainless steel, grade 1.4401), which produced an elastic compliance of 71 mm/N. The forces generated by the tissues were computed using the spring constant and the movement of a tiny magnet positioned at the spring wire's free end. An embedded 3D sensor (FXOS8700, NXP Semiconductors, USA) detected the magnetic field generated by the magnet. The posts used for EHT mounting were covered with polyethylene tubes (0.96 mm outside diameter, Portex, Smiths Medical, Dublin, USA) with a flattened bottom end to guarantee solid tissue support. Bipolar, current-controlled electrical pulses with a length of 2 × 1 ms, an amplitude of 50 mA, and a frequency of 1 Hz (60 bpm) were used to stimulate the EHTs. The graphite electrodes (6 × 8 mm^2, CG1290, CGC Klein, Germany) were positioned on either side of the EHTs to apply the electrical pulses (Figures 8A and 8C). An array of eight BMCCs was mounted onto a gearless stepper motor-driven rocking platform and operated using a specialized microcontroller (NXP K22F) for autonomous stimulation and continuous force measurement (Figure 8B). The integrated rocker mechanism tilted the BMCCs at a 12° angle and 60 rpm around their longitudinal axis, reducing heat dissipation in the CO_2-incubator and promoting oxygen uptake. The medium's PO_2 levels were maintained between 70-100 mmHg using this approach. The culture system was maintained in a standard incubator (at 37 °C, 3% CO_2, and 80% humidity) and connected to an external computer via USB, which ran custom software for stimulation control and data acquisition (Figure 8C). The forces generated by the tissues were measured at 2 ms intervals and stored for subsequent analysis. Further analysis of the data was performed using LabChart Reader software (ADInstruments, Australia).

The primary EHTs were moved from organotypic filters to BMCCs that had been pre-warmed to 37 °C with 2.4 mL of modified EHT culture media(72) (Table 2). The EHTs were placed in the BMCCs by puncturing their centers with neighboring holding posts, which were then adjusted to a 3 mm spacing to form a ring-shaped EHT that was immediately subjected to electrical stimulation (1 Hz, 50 mA current) and stretch conditioning. To promote EHT maturation and minimize the risk of damage (as demonstrated in our prior work(35)), the EHTs were distended once a day by manually moving the sliding fixation hook (adjustable post) at a rate of 0.16 mm/day for three

days. The medium was partially exchanged every other day (with 1.6 mL of fresh medium), which included the addition of 0.1 nmol/L 3,3′,5-triiodo-L-thyronine (Sigma-Aldrich).

Eight independent experiments from two clones were conducted, and EHTs were cultured for 7 days. On the final day of cultivation, various parameters such as contractility and spontaneous beating frequency of EHT under distinct conditions were evaluated.

Table 2 50 ml EHT medium composition

Reagents	Stock	Volume
B27- Insulin (Gibco, A1895601)	100 X	1 ml
MEM Non-Essential Amino Acids Solution (Gibco, 11140050)	100 X	0.5 ml
Penicillin/Streptomycin	100 X	0.5 ml
Dexamethasone (Sigma Aldrich, D4902)	-	5 µl
IGF-1 (PEPROTECH ,100-11)	0.5 µg/µl	10 µl
FGF-2 (PEPROTECH, 100-18B)	0.1 µg/µl	5 µl
VEGF165 (PEPROTECH, 100-20)	0.1 µg/µl	2.5 µl
TGF-ß1 (PEPROTECH,100-21)	0.1 µg/µl	2.5 µl
IMDM (Gibco, No. 12440061)	1X	50ml

IMDM indicates Iscove's Modified Dulbecco's Medium; DMEM/F-12 indicates Dulbecco's Modified Eagle Medium/Nutrient Mixture F-12; EHT, engineered heart tissue; FGF-2, fibroblast growth factor-2; IGF-1, insulin-like growth factor 1; TGF-β1, transforming growth factor-β1; VEGF165, vascular endothelial growth factor 165.

Response to increasing contraction frequency:

Contraction frequency was altered by modulation of the frequency of electrical stimulation in EHTs. EHTs were electrically stimulated at 1.0 Hz under baseline conditions. In the 1.5 Hz group, electrical stimulation frequency was gradually increased from 1 Hz by 0.1 Hz per minute until the frequency of 1.5 Hz was reached. In the 3.0 Hz group, electrical stimulation frequency was gradually increased from 1.0 Hz by 0.2 Hz per minute until the frequency of 3.0 Hz was reached. After a lapse of 72 hours, the electrical stimulation frequency for all groups was readjusted to 1.0 Hz.

Hypoxia:

For induction of tissue hypoxia, medium agitation was stopped for a 2-minute interval. Electrical stimulation was maintained at 1.0 Hz and contraction force recording was continued throughout.

Response to beta-adrenergic stimulation:

Incremental concentrations of the non-selective beta-adrenoceptor agonist isoprenaline (10^{-9} to 10^{-6} M in Tyrode solution) were added into the BMCC in 2 hours intervals. Contractile force was continuously recorded. Drug-induced changes in generated force, beating frequency, relaxation duration, and contraction duration were determined.

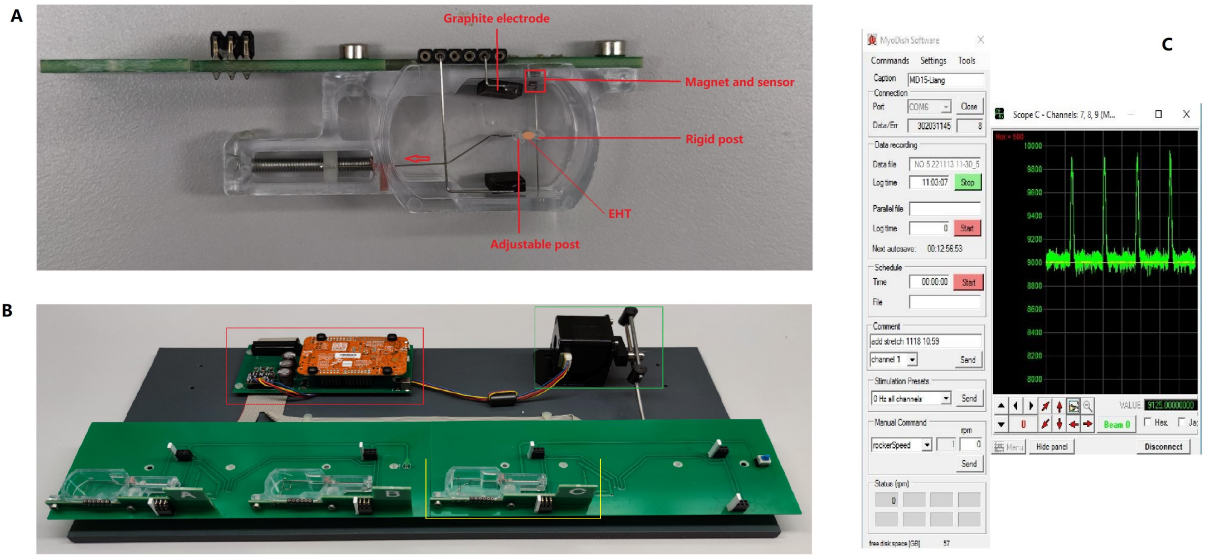

Figure 8. Introduction of the biomimetic culture chamber (BMCC) system(35).

A. Schematic diagram of the mechanical principle of the BMCC. The red arrows indicate the stretching direction.

B. The hardware system and BMCC connection. A micro-controller (Upper left red box) collects contraction data, generates stimulation pulses, and controls the rocking of the BMCC (Lower yellow box) platform by a stepper motor (Upper right green box).

C. The software system manages the system and collects data. A control panel (left) was used to configure data storage and stimulation parameters. EHT contractile forces were shown (right), and each peak represents one systolic-diastolic cycle.

2.2.6 Quantitative real-time PCR analysis

RNA extraction was carried out with the RNeasy Mini Kit (Qiagen). RNA integrity number (RIN) was determined using Simplinano Spectrophotometer (Biochrom). Equivalent amounts of RNA were reversely transcribed using the QuantiTect Reverse Transcription Kit (Qiagen), according to the manufacturer's instructions. All qRT-PCR analyses were conducted in duplicate on a StepOnePlus Real-Time PCR System (Applied Biosystems), with the following cycling conditions: a holding stage at 95 °C for 10 min, followed by 40 cycles at 95 °C for 15 s, 60 °C for 1 min, and 72 °C for 15 s. The gene expression results were analyzed using the $2^{-\Delta\Delta CT}$ method, and glyceraldehyde-3-phosphate dehydrogenase (GAPDH) was used as an endogenous control for mRNA expression. A primer list is available in Table 3 and Table 4.

Table 3 Primer list for RT-qPCR (Human)

Gene	forward	reverse
GAPDH	GGTCTCCTCTGACTTCAACA	AGCCAAATTCGTTGTCATAC
TBX5	ACACATCGTGAAAGCAGACG	TAACTCCAGGTCATCACTGC
NKX2.5	CCAAGGACCCTAGAGCCGAA	ATAGGCGGGGTAGGCGTTAT
MEF2C	CCAACTTCGAGATGCCAGTCT	GTCGATGTGTTACACCAGGAG
MYH7	ACTGCCGAGACCGAGTATG	GCGATCCTTGAGGTTGTAGAGC
HAND1	GAGAGCATTAACAGCGCATTCG	CGCAGAGTCTTGATCTTGGAGAG
Connexin-43	GGGACAGCGGTTGAGTCAG	TGTTACAACGAAAGGCAGACTG
ISL1	ATGGGAGACATGGGAGATCCA	GCATTTGATCCCGTACAACCTGAT
TBX20	TCACTGTCCGTAGTTCCGC	CCACAAATTGCTCCAGGGGT
CORIN	GCCGGTCTTGAGAGCTGAT	GTTCATACAGGCACCAACATAG
GATA4	GCCCAGCAGGACCCC	CTATTGGGGGCAGAAGACGG
cTnT	AGACAGAGCGGAAAAGTGGG	TCCTTGGCCTTCTCCCTCAG

Table 4 Primer list for RT-qPCR (Swine)

Gene	forward	reverse
GAPDH	ACACTCACTCTTCTACCTTTG	CAAATTCATTGTCGTACCAG
TBX5	AGGTGGGATTTTTGGAGAGCA	TCGGGTTTTGAGTCACAGGG

TBX20	CGTGGACAACAAGAGGCTGT	CAGTGAGGCTGTGTGGTCTT
CORIN	GAGCGAAAAGCAAGGCATCC	CAGCTCCCAAGACCCGC

2.2.7 RNA Sequencing of EHTs

Messenger RNA was purified from total RNA of 3 EHTs per group using poly-T oligo-attached magnetic beads. After fragmentation, the first strand cDNA was synthesized using random hexamer primers, followed by the second strand cDNA synthesis using either dUTP for directional library or dTTP for non-directional library. The library was checked with Qubit and real-time PCR for quantification and bioanalyzer for size distribution detection. Quantified libraries were pooled and sequenced on Illumina platforms, according to effective library concentration and data amount. Raw data (raw reads) of fastq format were first processed through in-house perl scripts. FeatureCounts(73) v1.5.0-p3 was used to count the reads numbers mapped to each gene. Then FPKM of each gene was calculated based on the length of the gene and reads count mapped to this gene. Differential expression(74) analysis was performed using the DESeq2Rpackage (1.20.0). Gene Ontology(75) (GO) enrichment analysis of differentially expressed genes was implemented by the cluster Profiler R package. GO terms with corrected P-value < 0.05 were considered significantly enriched by differential expressed genes.

2.2.8 Immunofluorescent staining

Whole cells or tissues were fixed in 4% paraformaldehyde (PFA) for 2 hours after being rinsed three times with phosphate buffer saline (PBS). Cells and EHTs were immersed in 1 mL of a 30% sucrose solution in PBS overnight at 4°C. Subsequently, cells and EHTs were washed for 30 minutes in PBS and permeabilized for 60 minutes in PBS containing 1% Triton X-100. The cells were then treated in a blocking solution (3% bovine serum albumin and 1% fetal calf serum in PBS) for 1 hour. The primary monoclonal anti-α-actinin antibody (sarcomeric, 1:100, Sigma-Aldrich) was incubated overnight at 4°C in antibody dilution buffer. The following day, samples were treated for 2 hours in antibody dilution buffer with goat anti-mouse IgG (H+L) and a highly cross-adsorbed secondary antibody, Alexa Fluor 546 (Invitrogen) at 1:100. Subsequently, cells and tissues were washed with PBS three times for 10 minutes and incubated overnight at 4°C with DAPI (2 µmol/L, Invitrogen).

2.2.9 Quantitation and statistical analysis

Data are shown as the mean +/- standard error of the mean (SEM). Comparative analysis of single cell data from the GSE106118 dataset, represented by median and interquartile range. To confirm the difference between groups, One-way ANOVA and Student's t test were used to test for treatment effects, as appropriate. GraphPad Prism 9 was used for all statistical analyses. Statistical significance was recognized at a threshold of error of $P < 0.05$. The number of independent experiments performed for each data set was detailed in the figure legends.

3. Results

3.1 RA signaling and determination of left and right ventricular marker genes in fetal heart

3.1.1 RA signaling genes expression in fetal heart

In order to determine a potential role for RA signaling in LV/RV differentiation, single cell RNA sequencing data from fetuses aged 5-7 weeks (start of cardiac contraction) were extracted from the GSE106118 dataset (Figure 9A) and further analyzed, separating the LV dataset and RV datasets. Principal component analysis combined with t-distributed stochastic neighbor embedding (t-SNE) showed the distribution of various cell types in the RV and LV being noticeably different (Figures 9B and 9C). Consistent with a role for RA signaling in differentiation into RV versus LV, expression of genes involved in RA signaling (RARA, RARB and the polycomb repressor 2 subunit SUZ12) was higher in fetal CMs of the LV as compared to the RV (Figure 9D).

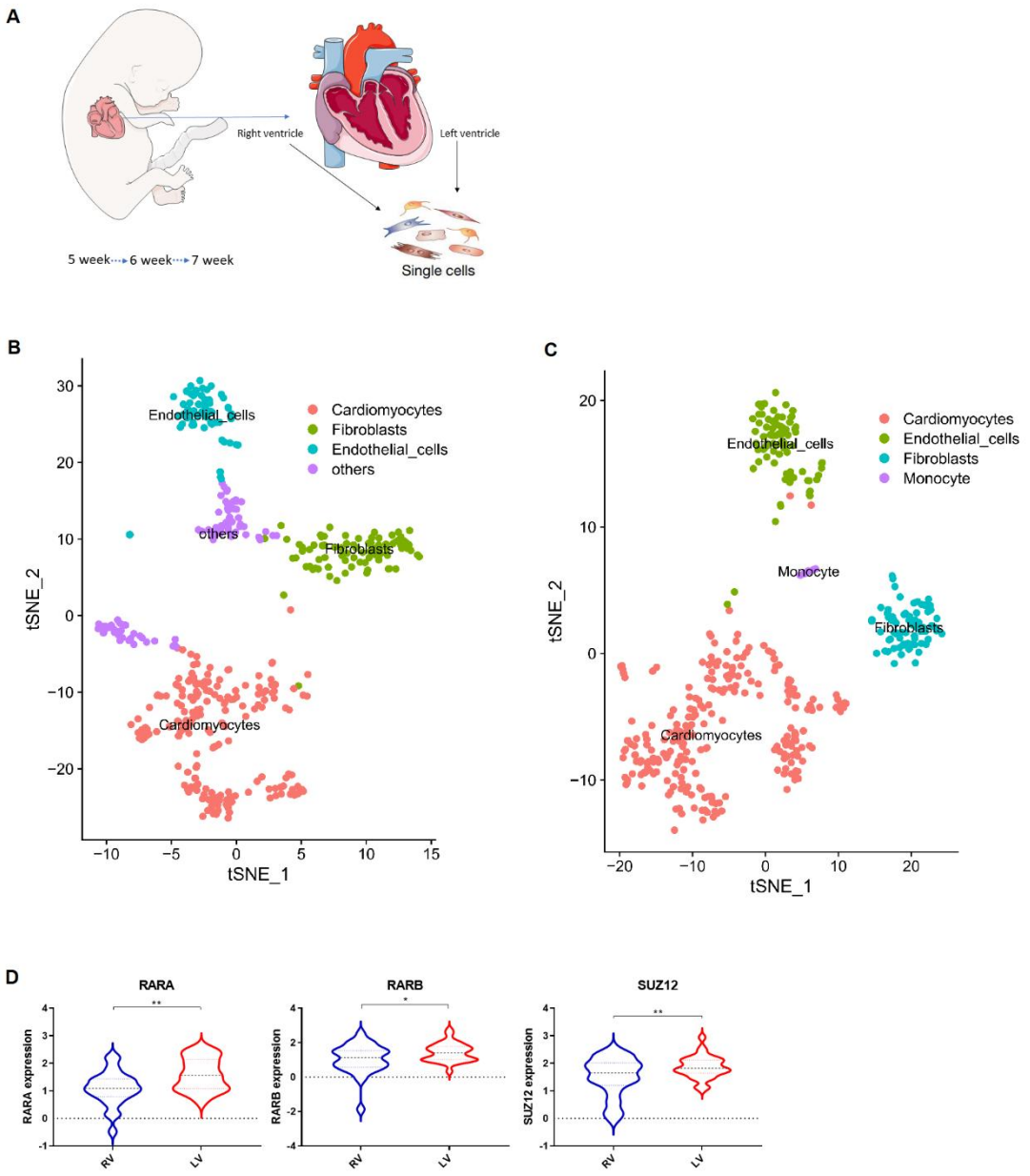

Figure 9. RA signaling genes expression in fetal heart.

A. Introduction to the GSE106118 single cell dataset. Single cell isolation from fetal heart ranging from 5 to 7 weeks.

B. t-SNE map shows the spatial distribution of transcriptome in different cell types of RV.

C. t-SNE map shows the spatial distribution of transcriptome in different cell types of LV.

D. The genes involved in the RA signaling pathway shows high expression in left ventricular cardiomyocytes. Unpaired t-test between LV and RV. *$p < 0.05$, **$p < 0.01$. Exclude the samples which gene expression is 0 in the original data, and all values are converted by log10.

3.1.2 Left and right ventricular marker genes expression in fetal heart

SUZ12 is known to regulate expression of transcription factors in embryonic development(76, 77), hence, expression of transcription factors and enhancers (TBX5, TBX20, NKX2.5, MEF2C, GATA4, ISL1) was determined within the CM populations (Figure 10A). TBX5 and NKX2.5 revealed a significantly higher expression in LV as compared to RV CMs, with very limited expression in other cell types, whereas GATA4, TBX20 and ISL1 were higher expressed in the RV CMs as compared to the LV CMs. Expression of MEF2C and cardiospecific enzyme CORIN was higher in the LV compare to the RV CMs (Figures 10B and 10C).

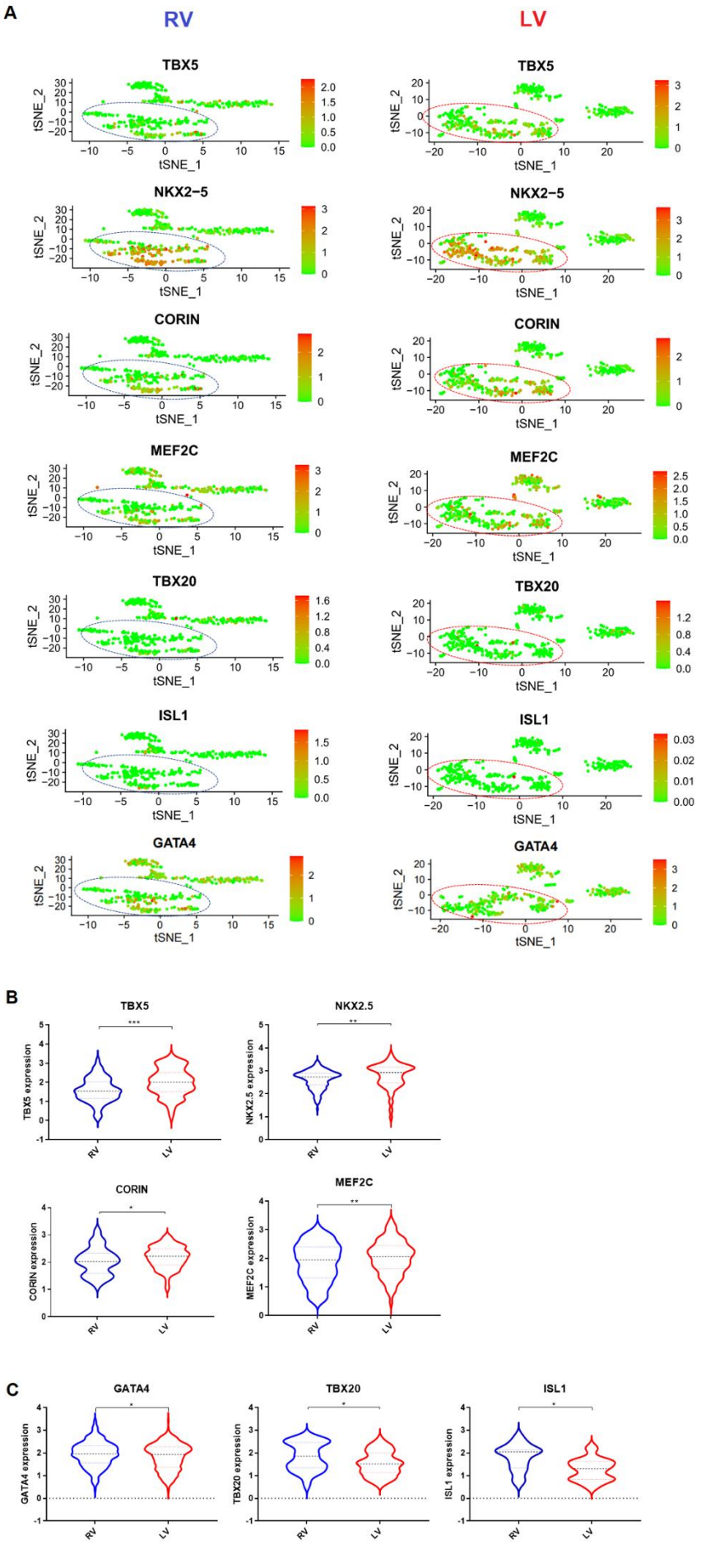
A
RV
LV
TBX5
NKX2−5
CORIN
MEF2C
TBX20
ISL1
GATA4
tSNE_1
tSNE_2
B
TBX5
NKX2.5
CORIN
MEF2C
TBX5 expression
NKX2.5 expression
CORIN expression
MEF2C expression
RV
LV
C
GATA4
TBX20
ISL1
GATA4 expression
TBX20 expression
ISL1 expression

Figure 10. Left and right ventricular marker genes expression in fetal heart.

A. Spatial distribution of marker genes in LV and RV. The blue circle represents the distribution area of right ventricular cardiomyocytes. The red circle represents the distribution area of left ventricular cardiomyocytes.

B. The marker genes of LV exhibited high expression in the left ventricular cardiomyocytes.

C. The marker genes of RV exhibited high expression in the right ventricular cardiomyocytes.

B and C: Unpaired t-test between LV and RV. *p < 0.05, **p < 0.01, ***p < 0.001. Exclude the samples which gene expression is 0 in the original data, and all values are converted by log10.

3.1.3 Validation of marker genes in adult human hearts

Expression levels of the above-mentioned genes as marker genes for LV and RV was further confirmed in adult human LV and RV. TBX5, NKX2.5 and CORIN showed a higher expression in human LV as compared to RV, while GATA4 and TBX20 showed a higher expression in RV as compared to LV (Figure 11). Surprisingly, MEF2C has a higher expression in human adult RV, although this may be part of the RV hypertrophic and/or stress response due to LV failure(78). ISL1, as a marker gene for right ventricular progenitor cells, was not expressed in adult hearts. Together with previous studies(36, 79), our data suggest that high expression of TBX5, NKX2.5 and CORIN can be used as marker of left ventricular CMs, whereas TBX20 ISL1 and GATA4 could be used to delineate right ventricular CMs.

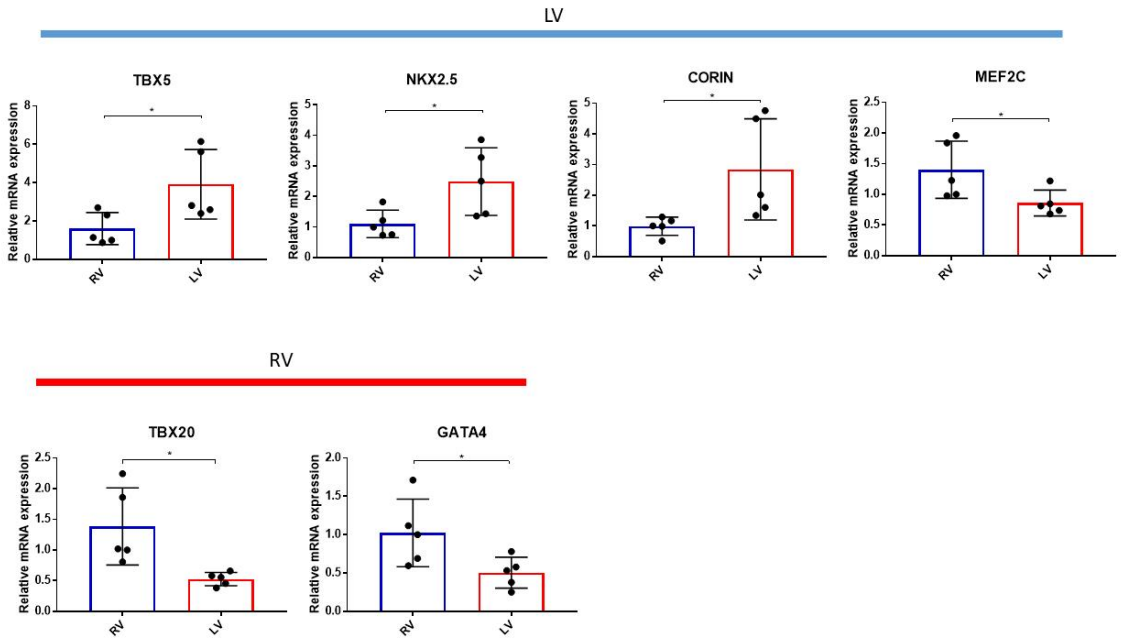

Figure 11. Expression of marker genes in adult humans.

*p < 0.05. Unpaired t-test between RV and LV.

3.1.4 Validation of marker genes in swine

In the case of TBX5 and CORIN, their expression was notably higher in the porcine LV in comparison to the RV, whereas the marker gene TBX20 displayed higher expression in the RV than in the LV (Figure 12). In adult porcine hearts, NKX2.5 and GATA4 exhibit negligible expression, leading us to speculate that these genes primarily function in regulating early cardiac development. Interestingly, ISL1 exhibited no differential expression between the left ventricle (LV) and right ventricle (RV) in either adult human or adult swine, implying that it serves as a marker for right ventricular progenitor cells.

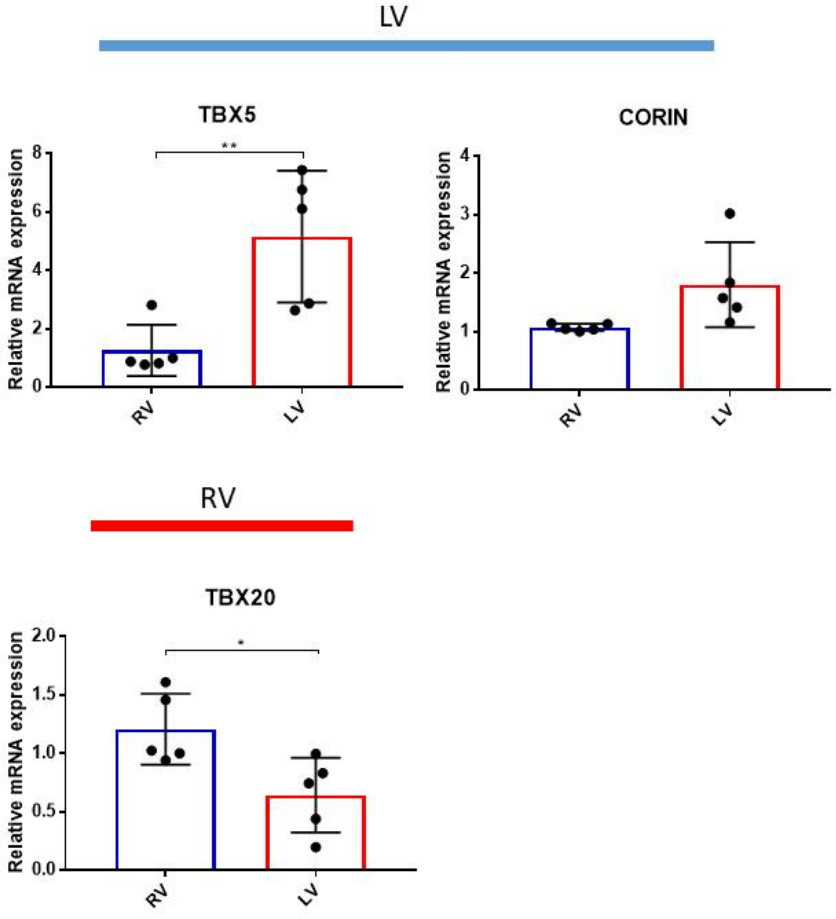

Figure 12. Expression of marker genes in swine.

*p < 0.05, **p < 0.01. Unpaired t-test between RV and LV.

3.2 Effect of RA on function of hiPSC-CMs

3.2.1 The function of hiPSC-CMs

The samples were categorized into three groups: the control group, the low RA (LRA) group, and the high RA (HRA) group, based on varying concentrations of RA intervention. A network of monolayers was established using standard stem cell culture and CM differentiation protocols. The initiation of beating in hiPSC-CMs occurred earlier in the HRA group (Figure 13A). Beginning on the 8th day of differentiation, the beating frequency of the cardiomyocytes was monitored. It exhibited a gradual increase, peaking on the 14th day of the differentiation process, followed by a gradual decline (Figure 13B). Remarkably, the HRA group displayed the highest beating frequency, achieving its peak ahead of the other groups (Figures 13B and 13C). Furthermore, the HRA group exhibited shorter contraction and relaxation times in comparison to the other two groups (Figure 13D).

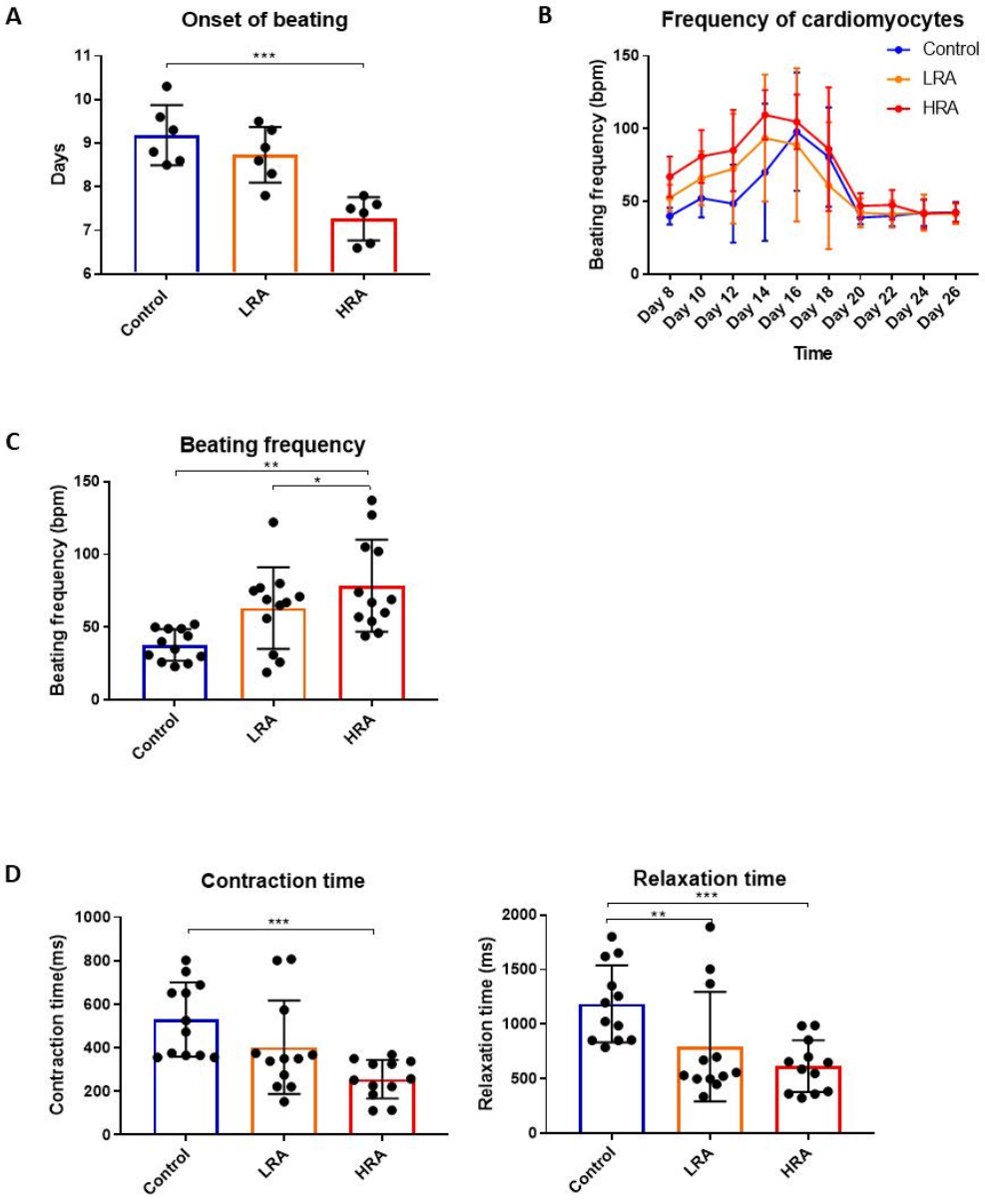

Figure 13. The basic function of hiPSC-CMs.

A. The onset of hiPSC-CMs beating time difference between groups.

B. The beating frequency of cardiomyocytes over time. The beating frequency was calculated every 48 hours from 8th day of differentiation, except for the samples that have the highest and lowest beating frequencies. n = 20.

C. The beating frequency of hiPSC-CM between groups.

D. The contraction time and relaxation time of hiPSC-CM between groups.

C and D: The time point for analysis was the 12th day of the differentiation process.

A, C and D: One-way ANOVA analysis, Tukey's multiple comparison test. *p < 0.05, **p < 0.01, ***p < 0.001.

3.2.2 The hiPSC-CMs response to isoprenaline

The hiPSC-CMs response to isoprenaline was examined. We observed that incremental concentrations of isoprenaline (Figure 14A) led to an increase in the beating frequency of cardiomyocytes, accompanied by a decrease in both contraction and relaxation times. As isoprenaline concentration increased, a reduction in the proportion of contraction time relative to the cardiac cycle was observed in the control group, along with a corresponding increase in the proportion of relaxation time (Figures 14B and 14C). There was little difference in the proportion of contraction and relaxation times relative to the cardiac cycle between the LRA and HRA groups as isoprenaline concentration increased.

Using basic functional analysis, we discovered that during the differentiation of hiPSCs into CMs, RA can modulate the function of CMs and their response to isoproterenol.

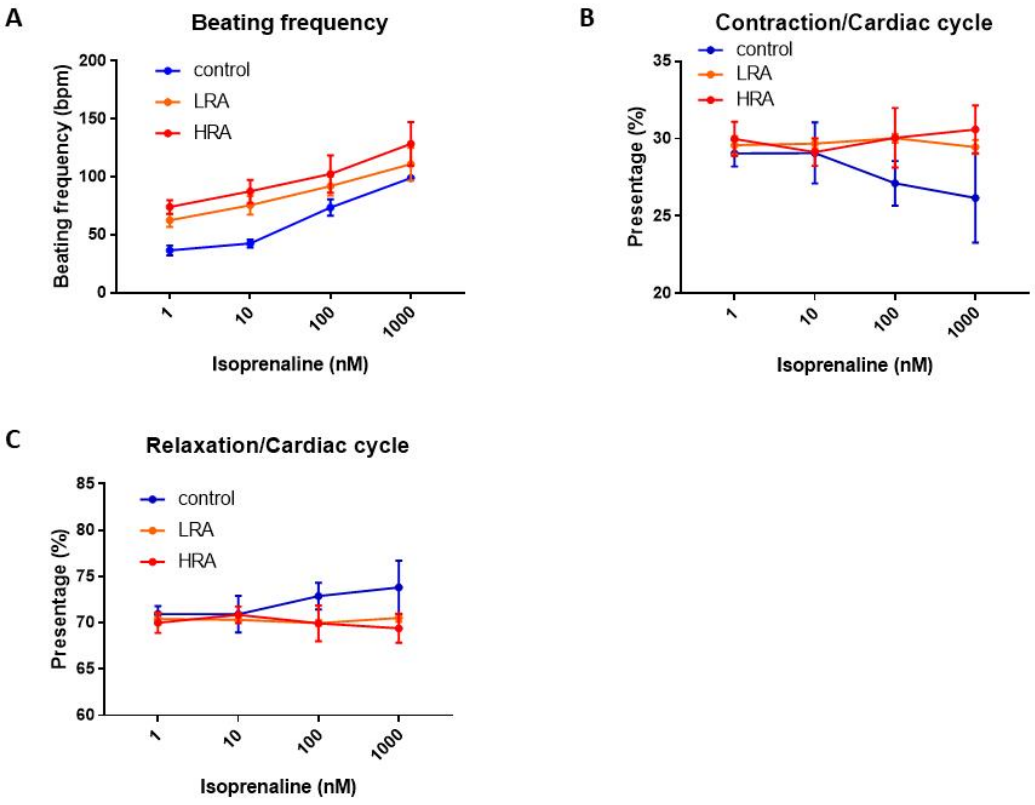

Figure 14. The hiPSC-CMs response to isoprenaline between groups.

A. The beating frequency in different concentrations of isoprenaline (n = 4).

B. The proportion of contraction time relative to the cardiac cycle in different concentrations of isoprenaline. (n = 4).

C. The proportion of relaxation time relative to the cardiac cycle in different concentrations of isoprenaline. (n = 4).

Isoprenaline was sequentially added to the well, starting with a low concentration and increasing to the next higher concentration every two hours.

3.3 Effect of RA on hiPSC-CM maturation and differentiation

3.3.1 RA promotes the hiPSC differentiation toward LV or RV like phenotype

Consistent with previous studies, iPSC culture and differentiation resulted in a network of CM monolayers, that started to beat spontaneously at day 6-9 of differentiation. On the 26th day of differentiation, hiPSC-CMs undergo maturation, and RNA was extracted from the cells for intergroup comparative analysis. Expression of transcription factors TBX5, NKX2.5, MEF2C and the enzyme CORIN was highest in the HRA group (Figure 15A). Conversely, expression of TBX20 and GATA4 was highest in the control group, whereas ISL1 showed the highest expression in LRA group (Figure 15B). These data suggest that RA in a concentration of 0.1μM promoted differentiation towards a LV phenotype via activation of TBX5, NKX2.5 and MEF2C, whereas RA concentrations $\leqslant$ 0.05 μM promote differentiation towards an RV like phenotype via activation of TBX20 and GATA4.

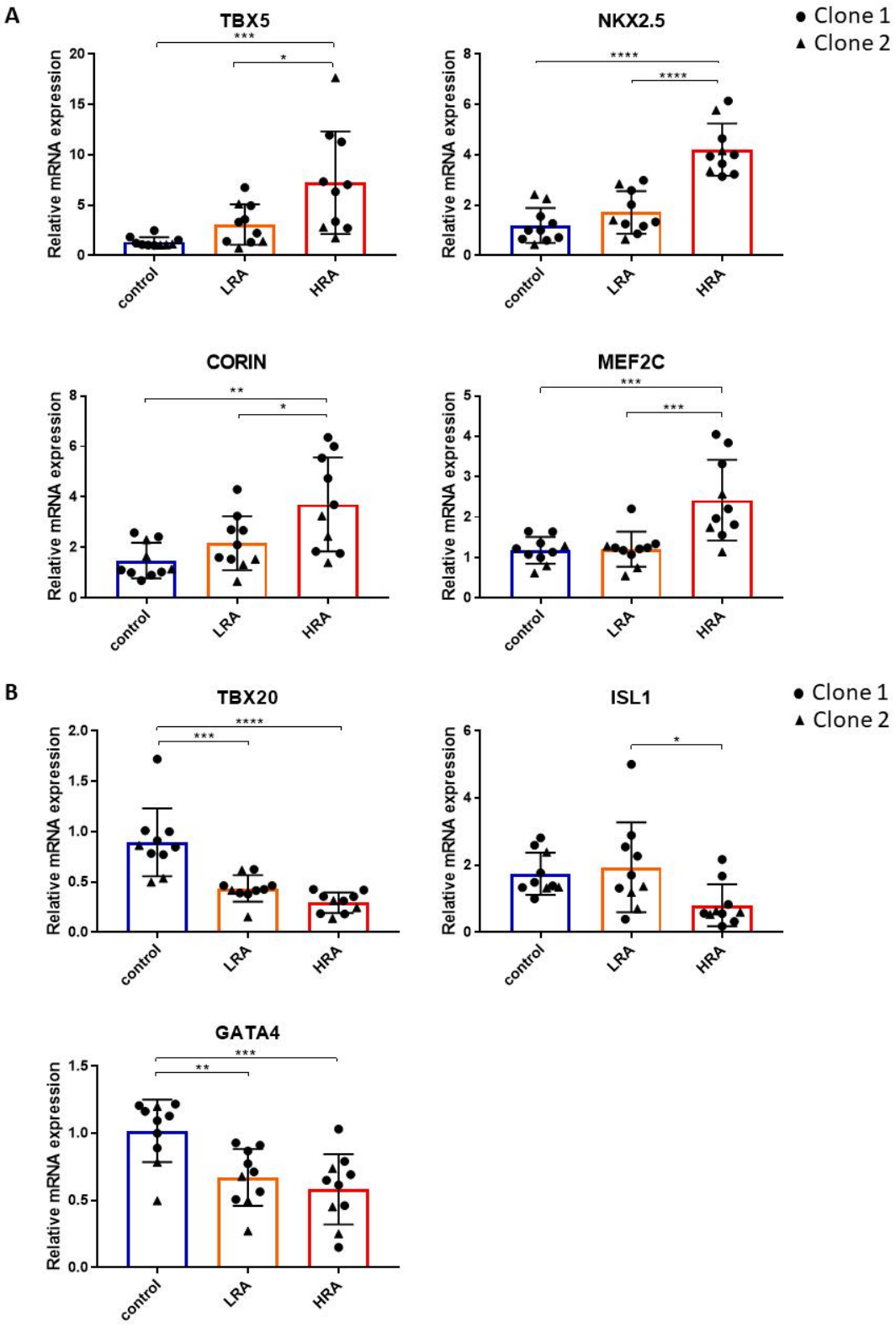

Figure 15. RA promotes the hiPSC differentiation toward LV or RV like phenotype.

A. Left ventricular marker genes expressed in hiPSC-CMs.

B. Right ventricular marker genes expressed in hiPSC-CMs.

Bar plots represent mRNA genes relative to glyceraldehyde 3-phosphate dehydrogenase (GAPDH) in control group, as determined by qPCR. One-way ANOVA, Tukey's multiple comparison test. *p < 0.05, **p < 0.01, ***p < 0.001, ****p < 0.0001.

3.3.2 RA promotes maturation of the iPSC-derived CMs

RA also promoted maturation of the iPSC-derived CMs, with more organized α-actinin expression in the HRA group (Figure 16A) and higher mRNA expression of cTnT and MYH7 in the HRA group as compared to control, whereas expression of connexin43 was not different (Figure 16B) at 26 days of differentiation and maturation.

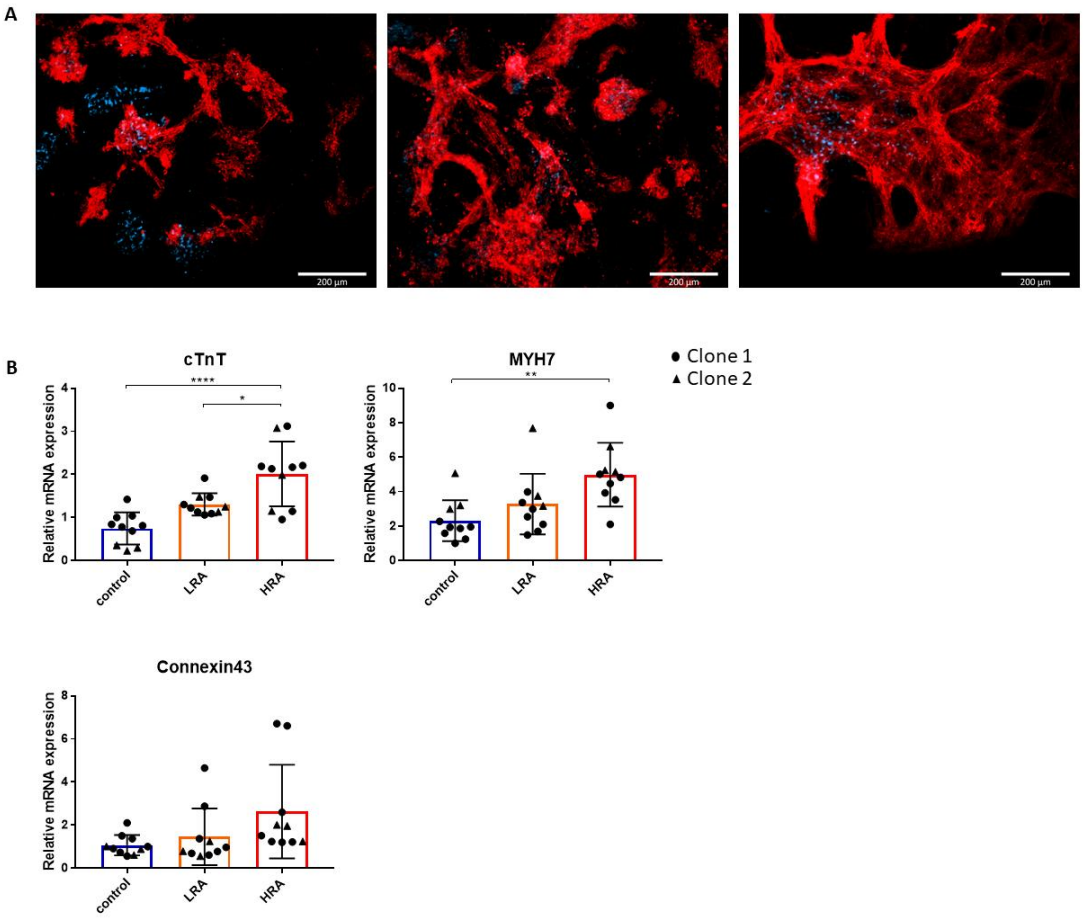

Figure 16. RA promotes maturation of the iPSC-derived CMs

A. α-actinin expression in hiPSC-CM. Left: control. Middle: LRA. Right: HRA. Immunofluorescent images of hiPSC-CM cultured for 26 days. α-actinin (red) and DNA (blue). Scale bar: 200 µm.

B. Relative mRNA expression of marker genes of CM maturation.

Bar plots represent mRNA genes relative to GAPDH in control group, as determined by qPCR. One-way ANOVA, Tukey's multiple comparison test. **p < 0.01, ****p < 0.0001.

3.4 Effect of RA on early iPSC differentiation persists in EHTs

3.4.1 RA promotes maturation of sarcomere in iPSC-derived EHTs

iPSC-derived CMs were further matured into EHTs, to assess whether the differences induced by RA persisted in this maturation step. Immunofluorescence staining revealed a high expression and organization of α-actinin within the HRA-EHTs, leading to enhanced sarcomere visibility (Figure 17).

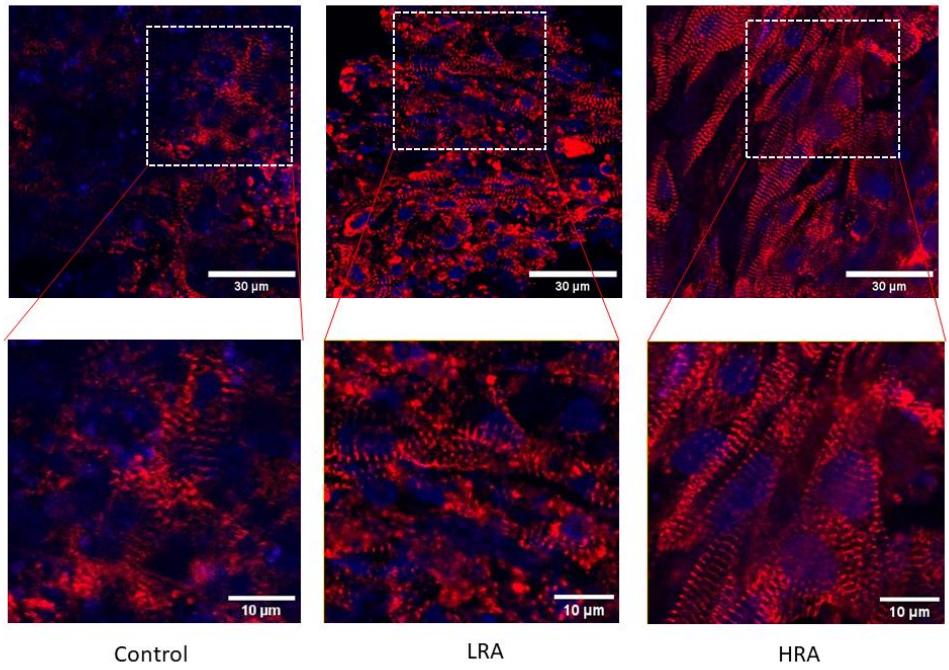

Figure 17. Immunofluorescence images of EHT across various experimental groups are presented.

Upper Panel: The spatial distribution of α-actinin exhibits variability across distinct EHT groups. Lower Panel: A localized magnification reveals variations in sarcomere quantity and quality within the different experimental groups.

3.4.2 Effect of RA on the maturation and differentiation of EHT

Consistent with the gene-expression in the iPSC-derived CMs, expression of TBX5, CORIN, MEF2C and NKX2.5 were highest (Figure 18A), while TBX20, GATA4 and ISL1 expression was lower in HRA-EHTs, as compared to control-EHTs (Figure 18B), after 7 days of maturation in the BMCC. Furthermore, markers of maturation and contractile function, cTnT, MYH7 and connexin 43 were highest in HRA-EHTs (Figure 18C).

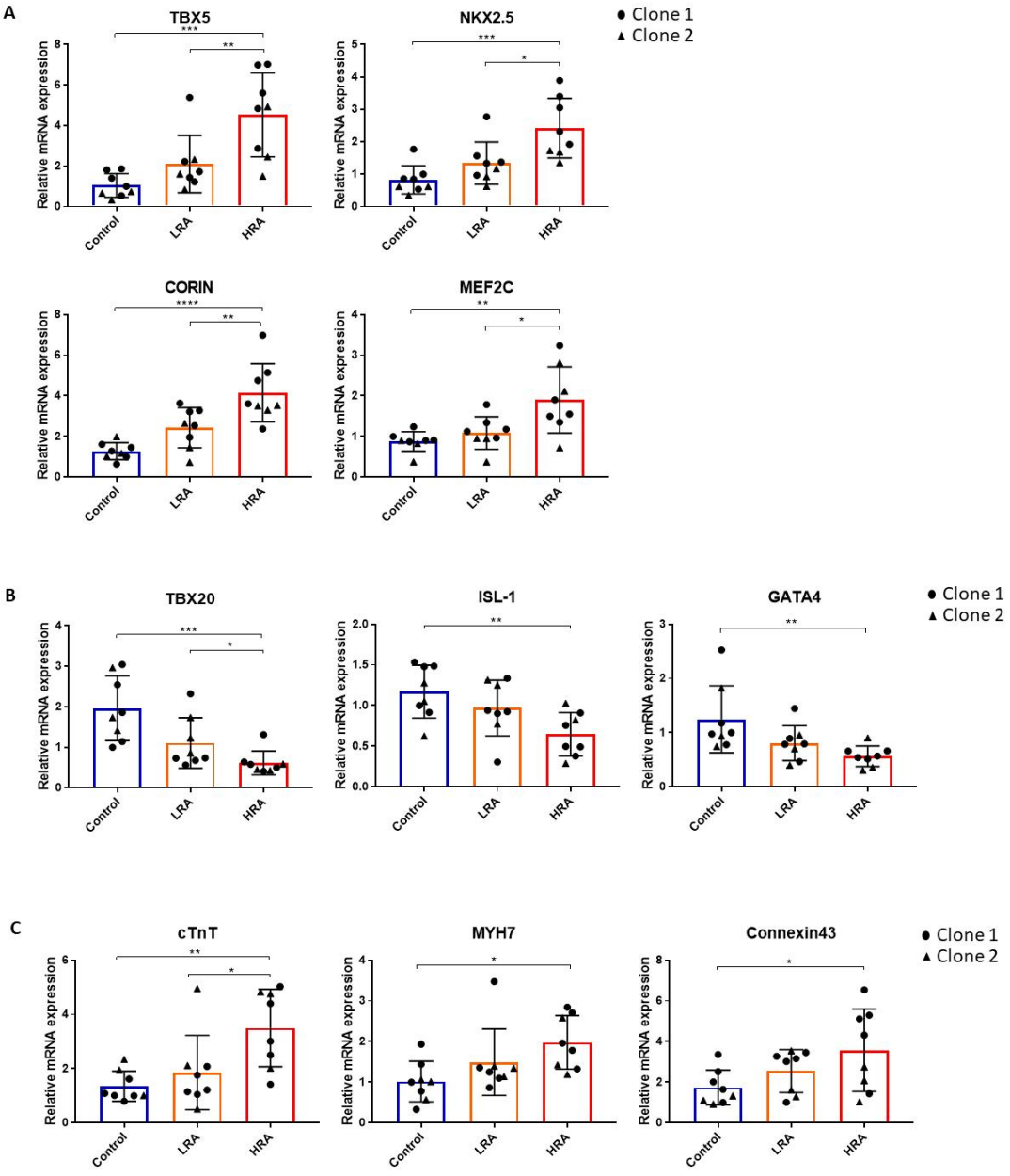

Figure 18. Effect of RA on the differentiation and maturation of EHT.

A. Marker genes of LV expressed in different groups of EHT.

B. Marker genes of RV expressed in different groups of EHT.

C. Marker genes of CM maturation expressed in different groups of EHT.

A-C: One-way ANOVA, Tukey's multiple comparison test. *p < 0.05, **p < 0.01, ***p < 0.001, ****p < 0.0001.

3.5 RA improves EHT maturity through altered gene-expression related to cell-cell and cell-matrix interaction

3.5.1 Comparison of mRNA sequencing results between the HRA group and the control group

To further investigate molecular changes underlying the improved organisation of the EHTs from CMs previously exposed to RA, RNA sequencing was performed. Data analysis revealed differentially abundant genes in the HRA-EHT compared to the control-EHT. We detected 110 and 690 genes upregulated and downregulated (p-value < 0.05 and fold change ≥ 1.3) in the HRA-EHTs respectively (Figure 19A). GO enrichment pathway analysis showed upregulation of several genes coding for the extracellular matrix (ECM) remodelling (SerpinB2, F3, TGFa), intermediate filaments and cell-cell junctions (CLD7, OCLN, PPL) (Figure 19B, table 5). Volcano plot analysis detected increased expression for several genes which play a vital role in cardiogenesis (Wnt6, BMP2, HOXA1) (Figure 19A)(46). Furthermore, the significant downregulated genes were primarily linked to the regulation of non-cardiomyocyte differentiation (Figure 19C, table 6). This suggests that, when compared to the control group, the HRA group demonstrates enhanced extracellular matrix and improved intercellular connections. Additionally, it implies that the presence of RA supports the differentiation of iPSCs into cardiomyocytes.

A

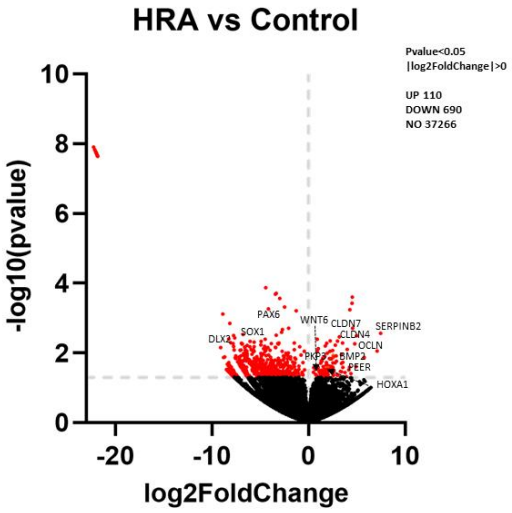

B

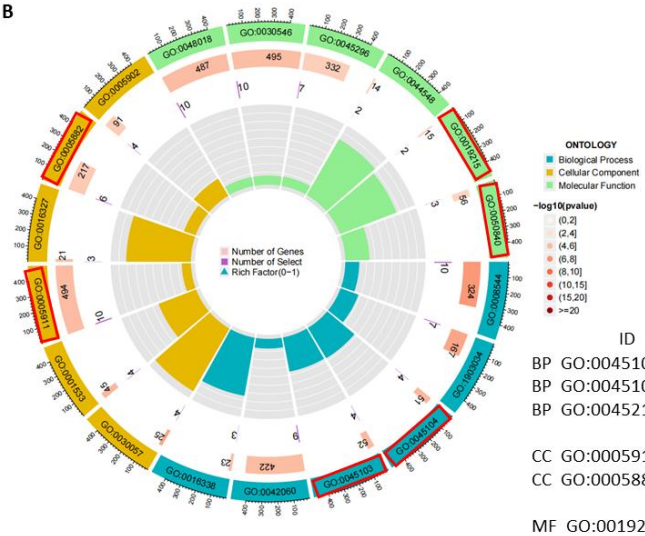

	ID	Description
BP	GO:0045104	Intermediate filament cytoskeleton organization
BP	GO:0045103	Intermediate filament-based process
BP	GO:0045216	Cell-cell junction organization
CC	GO:0005911	Cell-cell junction
CC	GO:0005882	Intermediate filament
MF	GO:0019215	Intermediate filament binding
MF	GO:0050840	Extracellular matrix binding

C

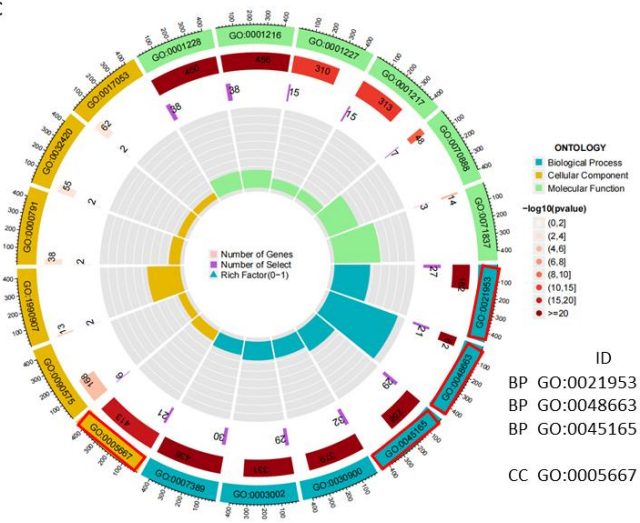

	ID	Description
BP	GO:0021953	Central nervous system neuron differentiation
BP	GO:0048663	Neuron fate commitment
BP	GO:0045165	Cell fate commitment
CC	GO:0005667	Transcription regulator complex

Figure 19. The DEGs between the HRA group and the control group.

A. Volcano map displaying DEGs between the HRA group and the control group.

B. GO terms illustrating the functional enrichment of upregulated DEGs between the HRA and control group.

C. GO terms illustrating the functional enrichment of downregulated DEGs between the HRA and control groups.

Table 5. List of significant upregulated genes (included in GO analysis) in the HRA compared to the control.

EPPK1	S100A6	GRHL3	AC110619.1	FHDC1	NTN4	SPP1	PRSS22
PXDNL	KCNG1	KRT81	C6orf132	BTG1	B3GNT4	TMEM191B	TMEM125
SEMA3D	TSPAN7	AL022157.1	SDC1	S100A11	TMEM54	ELF3	MAL2
SH3GLB2	KRT86	TMEM30B	SKAP2	SPTSSB	RHPN2	SYTL1	MGST1
EMP1	AC011365.1	MGAT3	C4orf19	FAM129B	PERP	ALX4	EPHA1
RAB9A	EPHB6	TNXB	STARD10	OCLN	WNT10A	NRADDP	MAB21L4
AC124947.2	OTUD1	NDRG2	MUC15	SYT4	CLDN4	KCNJ3	AC133644.3
EPS8L2	PGLYRP4	AC087071.1	NKPD1	F3	ABRACL	TGFA	PLEKHG6
WNT6	AC095055.1	MYO6	PTPN3	ZNF385B	VAMP8	TMEM184A	TACSTD2
WFDC21P	RBM47	MAPK13	GABRB3	PRRX2	CDS1	ENDOU	ARTN
HOTAIRM1	BMP2	PKP1	UPK1B	C2orf88	L1TD1	TNXA	ESRP1
S100A9	SERPINB2	HOXA1	KRT17	CGA	RNF223	KLK6	FAM174B
MDFIC	KLF4	TGM1	PKP3	INSL4	GPRC5A	LYPD3	AC005532.1
PPL	VGLL1	ATG9B	CLDN7	CLIC3	SH2D4A		

Table 6. List of significant downregulated genes (included in GO analysis) in the HRA compared to the control

ID2	HNF1B	PTF1A	ISL2	POU3F2	GAD1	PVALB	SIX3
HES3	HNF4G	HOPX	DBX1	NEUROG2	SATB2	DLX2	VSX2
NEUROD1	HNF1A	SOX14	LHX3	BARHL2	LHX6	NEUROD4	POU4F2
BHLHE22	ZNF503	SIM1	NKX6-2	ISL1	NEUROD6	EMX1	SIX6
TCF4	MAFA	RBPJL	FABP7	NEUROG3	TBR1	EMX2	LHX2
HES6	SSBP4	RFX4	LHX1	LHX5	NR4A2	SP8	OTX2
TCF12	SSBP3	RFX6	GSX1	ONECUT2	GSX2	FEZF2	POU4F1
VSX1	SSBP2	FEZF1	INSM1	LMO3	LMX1A	CALB2	PAX6
NHLH1	LHX4	MAFB	FOXA2	OTP	DLX1	FOXN4	NEUROG1
PRDM8	LDB1	PAX4	NKX2-2	NKX6-1	POU3F3	PITX3	SOX1
OTX1	LMO4	PDX1	ONECUT1	OLIG3	MYT1L	SOX11	LHX9
MSC	ID3	ZBTB18	SP3	TMEM215			

3.5.2 Comparison of mRNA sequencing results between the HRA group and the LRA group

We detected 37 and 1387 genes upregulated and downregulated (p-value < 0.05 and fold change ≥ 1.3) in the HRA-EHTs as compared to the LRA_EHTs respectively (Figure 20A). In the HRA-EHTs vs LRA-EHTs, upregulated genes were associated with response to RA and intermediate filaments (Figure 20B, Table 7), which have a close connection with myocardial tissue dilation, mitochondrial dysfunction, and diminished contractile capabilities(80).

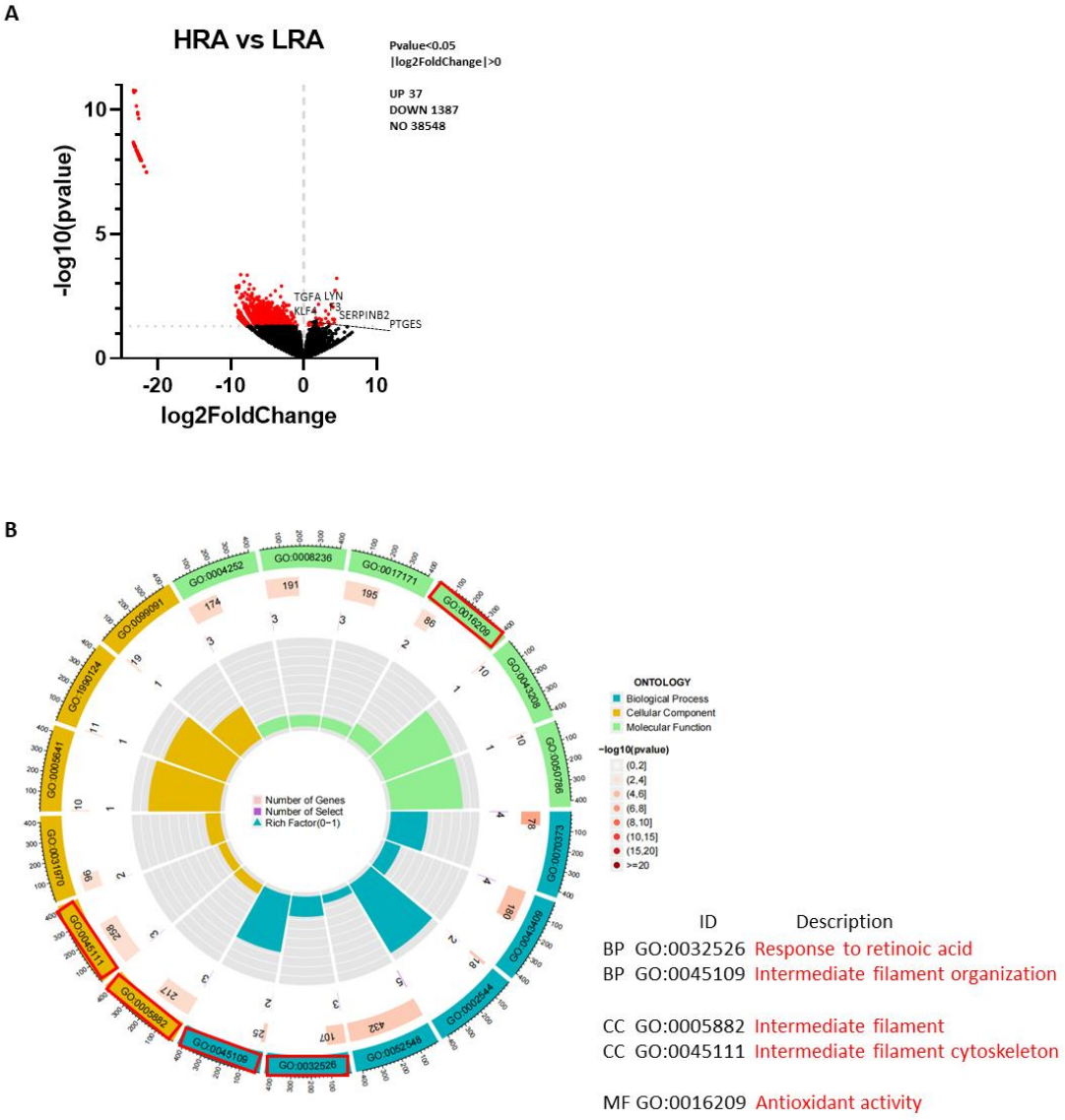

Figure 20. The DEGs between the HRA group and the LRA group.

A. Volcano map displaying DEGs between the HRA group and the LRA group.

B. GO terms illustrating the functional enrichment of upregulated DEGs between the HRA and the LRA group.

Table 7. List of significant upregulated genes (included in GO analysis) in the HRA compared to the LRA

KLK6	FSTL5	PTGES	AC011365.1	AHNAK2	F3	SERPINB2
HIST1H2BD	ELF3	LYPD3	MXI1	KLK1	TCEA1P2	S100A9
NFIL3	MPZL3	LYN	TMEM196	PSCA	TGFA	NXPH4
C6orf132	KRT6B	SLC39A2	NDRG2	RHOD	SGPP2	PKP1
ITSN2	GALNT3	TNFSF9	KLF4	TNXA	PGLYRP4	KRT17
PWWP2B	EMP1					

3.5.3 Comparison of mRNA sequencing results between the LRA group and the control group

311 and 43 genes were upregulated and downregulated (p-value < 0.05 and fold change ⩾ 1.3) in the LRA-EHTs vs Control-EHTs respectively. The GO enrichment pathway analysis did not reveal any significant pathway-changes between these two groups. However, we did observe upregulation of transcription factors (FOSl1, FOSB, HOXA5) using a volcano plot analysis (Figure 21). Thus, both the comparisons (HRA vs Con and LRA vs Con) identified that RA treatment affected expression of HOX genes. This is a significant finding as HOX genes play a critical role during heart development(81) and several of these Hox genes feature RA-response elements (RAREs) in their enhancers or proximal promoters(82).

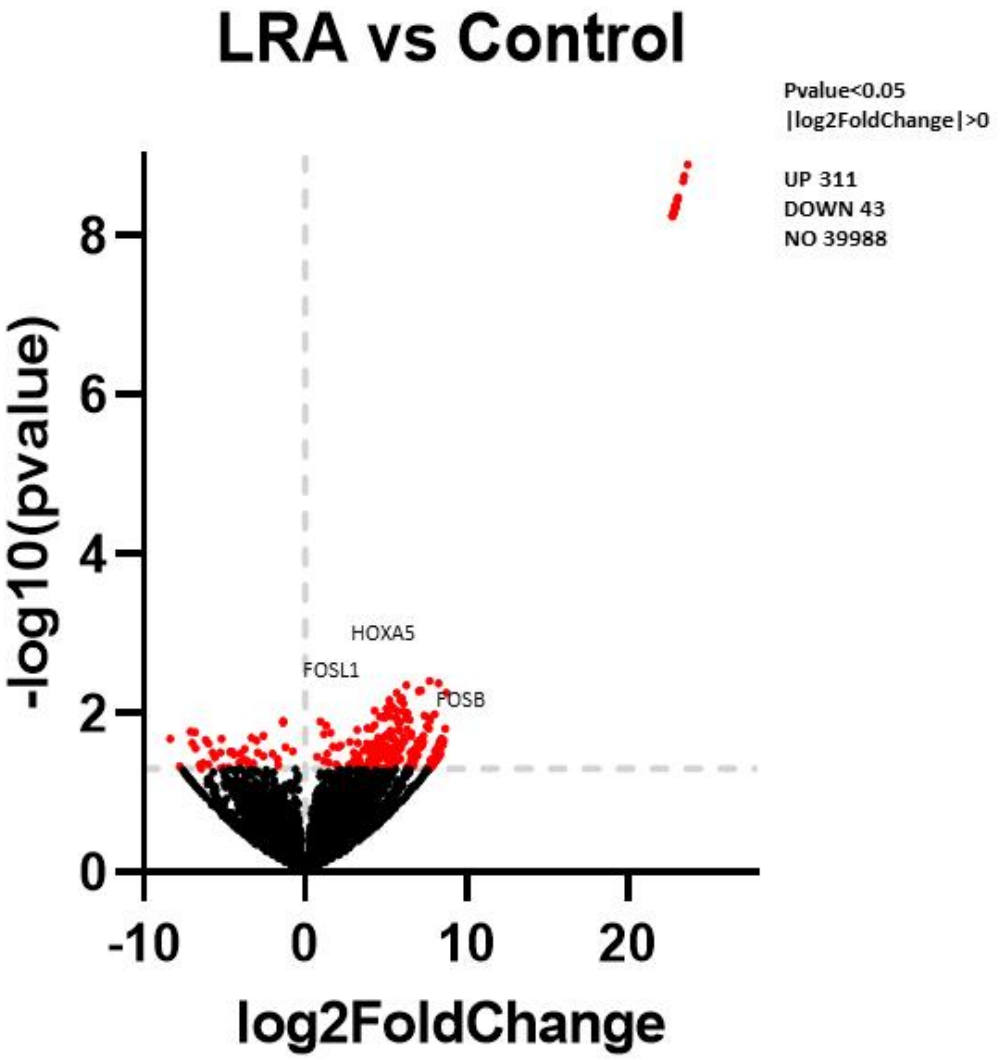

Figure 21. Volcano map displaying DEGs between the LRA group and the control group.

3.5.4 PPARG as the central hub gene connecting RA and cell-matrix interaction

In order to unravel the relationship between the RA pathway, transcription factors, intermediate filaments, extracellular matrix genes, and HOX genes, we performed a protein-protein interaction (PPI) network analysis. This analysis was aimed at complementing our RNA sequencing data with published research. The network highlights PPARG as the central hub gene (Figure 22). Numerous groups have presented PPARG as a critical factor in cardiac development but its specific role in inducing left versus right ventricle warrants further studies(83, 84).

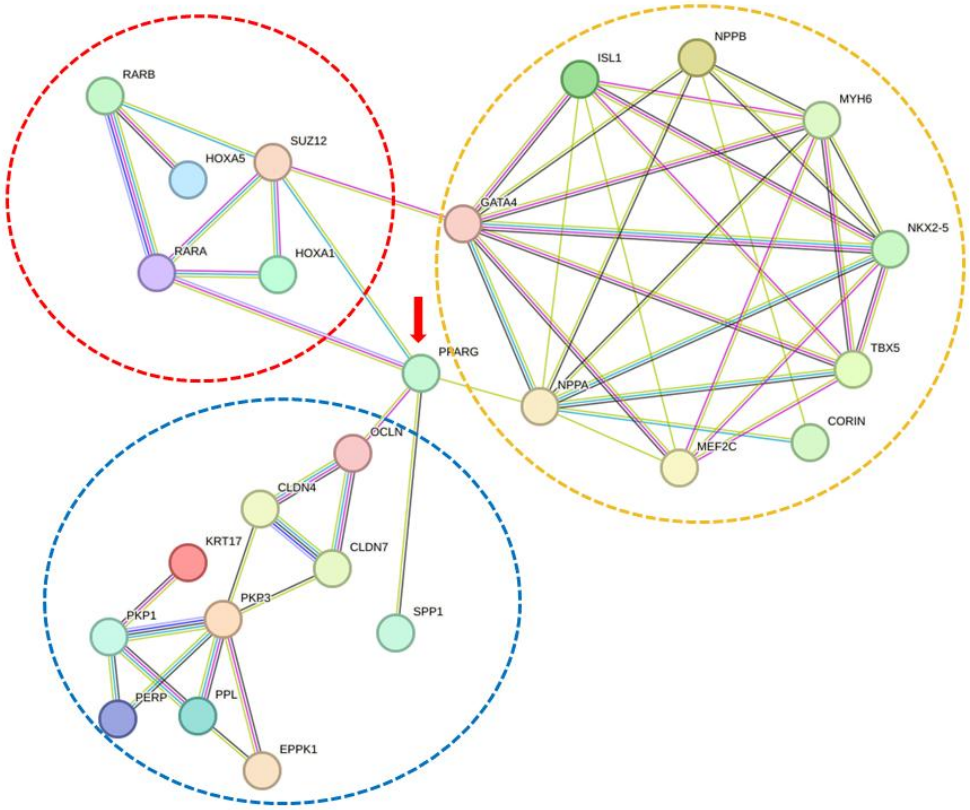

Figure 22. PPI network illustrating the relationship between RA signaling pathway, transcription factors and the extracellular matrix.

The red circle represents protein relevant to the RA signaling pathway. The yellow circle represents transcription factors relevant to ventricular differentiation. The blue circle represents proteins related to the extracellular matrix.

3.6 Effect of RA on EHT function

3.6.1 The contractility of EHT over time

As EHT matured in BMCC under the condition of constant preload, contractile force gradually increased over time in all groups, especially during the first three days when the preload was gradually increased (Figures 23A and 23B), while the contraction time and relaxation time showed no significant change (Figures 23C and 23D). In order to eliminate the influence of preload on the contractility, the contractility index (Contractile force/preload force) has been employed for comparing the strength of contractility between groups, and it has been found that the contractility of HRA-EHT was still the highest (Figure 23E).

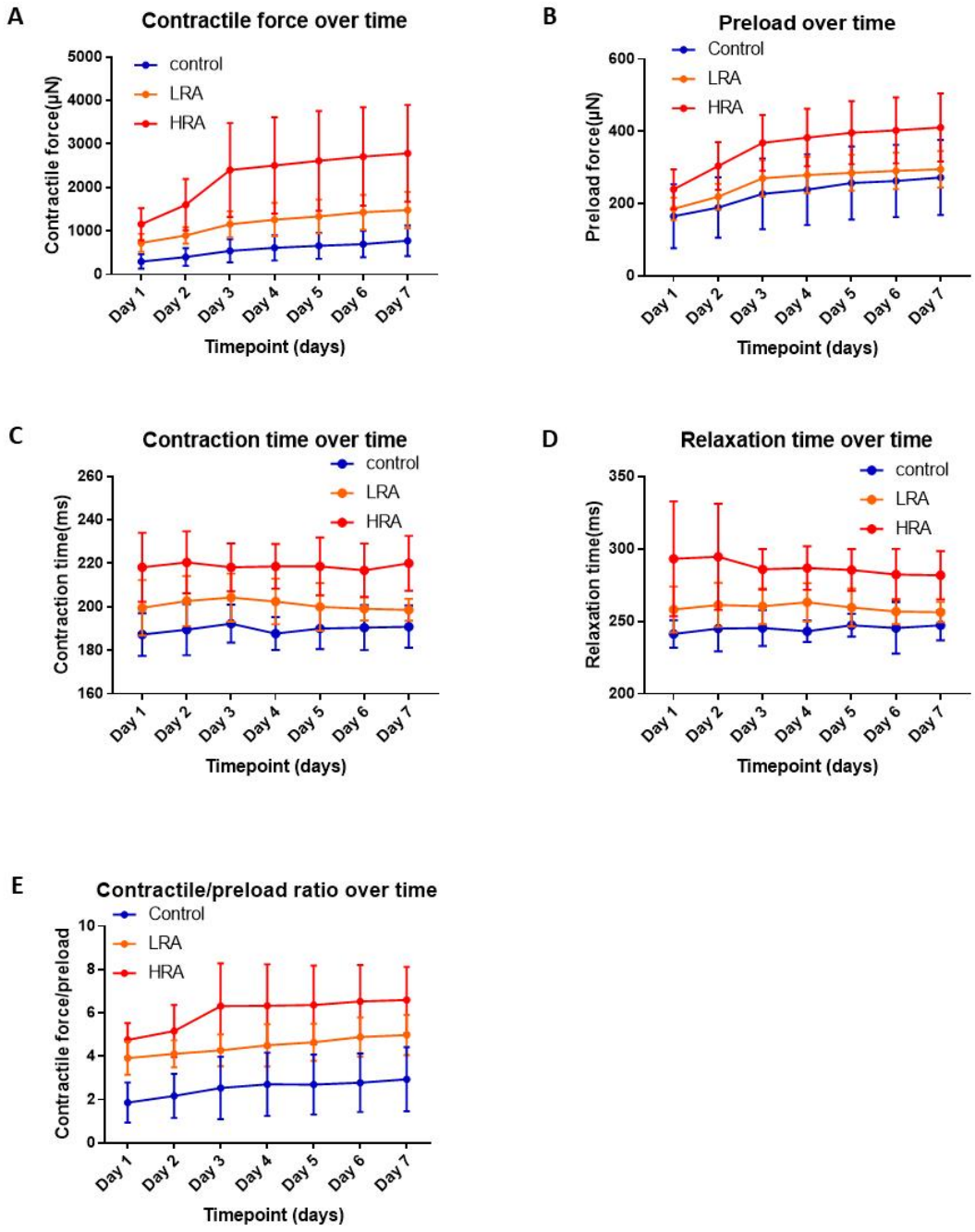

Figure 23. The contractility of EHT over time.

A. The contractile force of EHT over time. n = 11.

B. The preload force of EHT over time. n = 11.

C. The contraction time of EHT over time. n = 11.

D. The relaxation time of EHT over time. n = 11.

E. The contractile force/preload of EHT over time. n = 11.

3.6.2 The function of EHTs in different groups

On the fourth day in the BMCC, the supplemental preloading was discontinued, and the evaluation of EHT functionality among various groups commenced. We found that beating frequency was lower and contraction force was consistently higher in HRA-EHTs as compared to the LRA-EHTs and control-EHTs (Figures 24A and 24B), even after correction for a higher preload, using the contractility index (force/preload) (Figures 24C and 24D). The differences in gene expression induced by RA during hiPSC-CM differentiation translated into functional changes, that were persistently present.

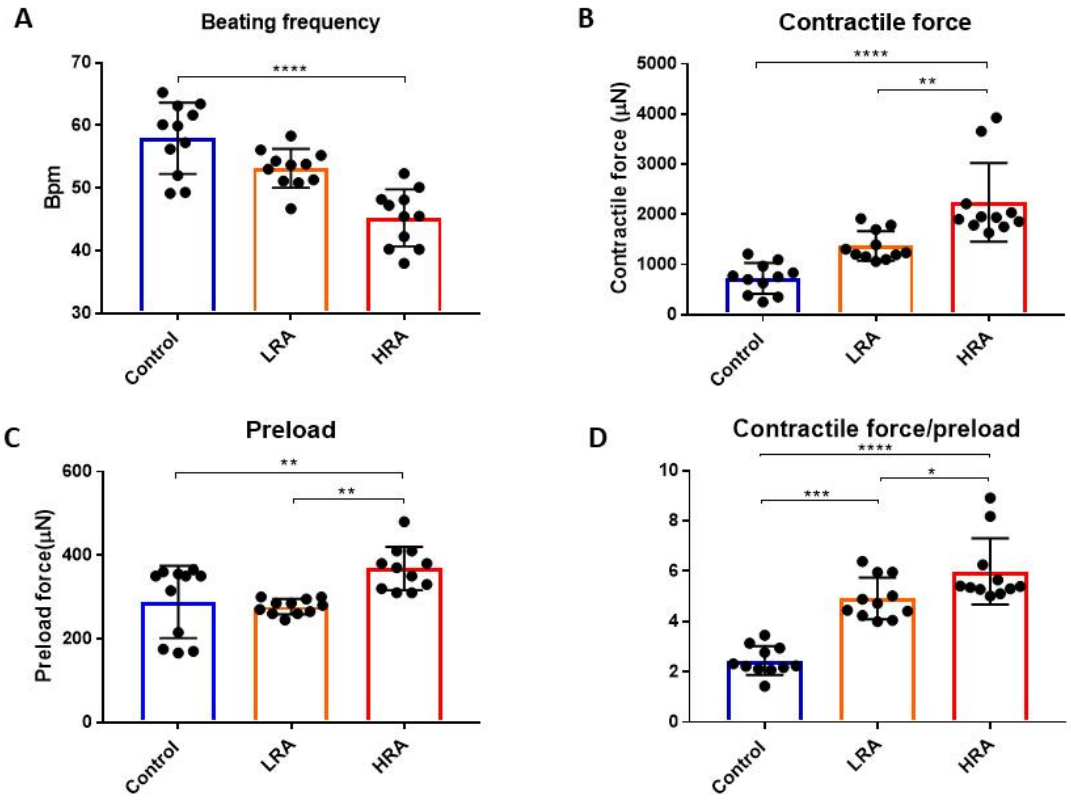

Figure 24. The function of EHTs after supplemental preloading was discontinued.

A. The beating frequency of EHTs between groups.

B. The contractile force of EHTs between groups.

C. The preload force between groups.

D. The contractile force/preload between groups.

All data analysis was conducted on the fourth day when supplemental preloading was discontinued. One-way ANOVA, Tukey's multiple comparison test. *p < 0.05, **p < 0.01, ***p < 0.001, ****p < 0.0001.

3.7 EHT response to stress

3.7.1 Hypoxia

The response of the EHTs to hypoxia was assessed by stopping the rocking of the BMCC system. The contractile force and beating frequency in HRA-EHTs were more sensitive to hypoxia as compared to the control-EHTs, while the LRA-EHTs showed an intermediate response (Figures 25A and 25B). These data are consistent with HRA-EHTs showing a more LV-like phenotype, as the LV has a stronger contractile force and higher oxygen consumption compared to RV(85, 86).

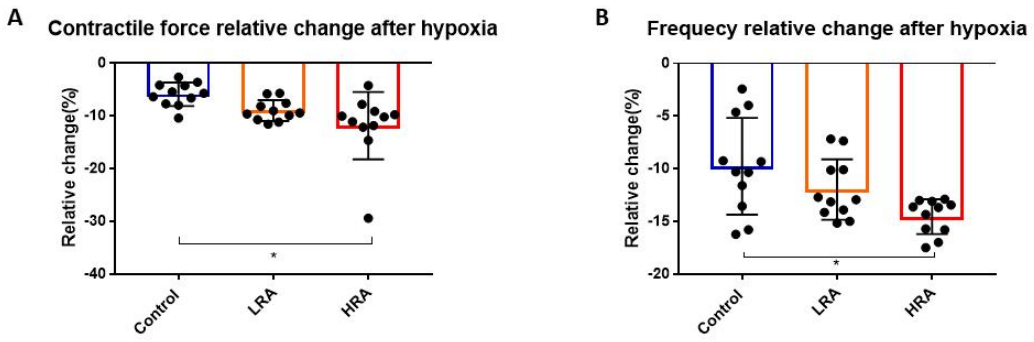

Figure 25. The response of EHTs to hypoxia.

A. The relative change of contractile force after hypoxia in different groups.

B. The relative change of beating frequency after hypoxia in different groups.

One-way ANOVA, Tukey's multiple comparison test. *$p < 0.05$.

3.7.2 β-adrenergic stimulation

The effect isoprenaline reached its peak approximately 10 minutes after administration and its effect lasted for up to 2 hours (Figures 26A and 26B). Therefore, we increased the concentration of isoprenaline in EHT medium every 2 hours. We found that the β-adrenoceptor agonist isoprenaline significantly increased the contractile force (Figure 26C) and beating frequency (Figure 26D) of the EHTs. The effect of β-adrenergic stimulation was most pronounced in the HRA-EHTs, consistent with observations that expression of β-adrenoceptors is highest in the LV(86). Altogether, these data confirm a LV-like phenotype of HRA-EHTs and a RV-like phenotype of EHTs from the LRA and control groups.

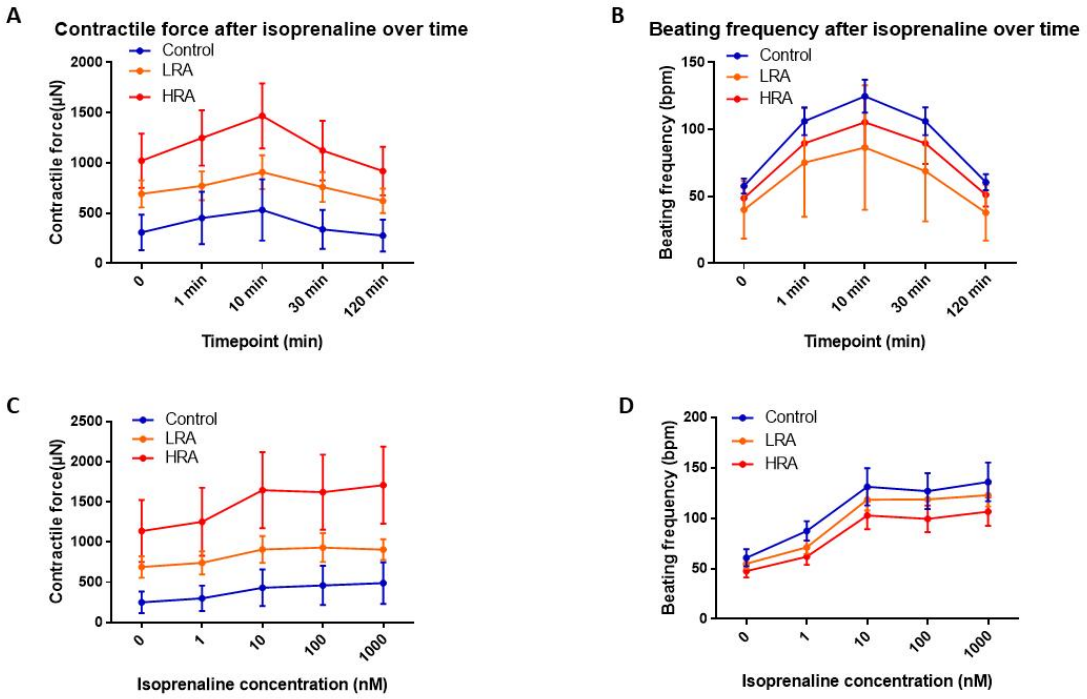

Figure 26. The response of EHTs to hypoxia isoproterenol.

A. Comparison of the duration and peak contractile force of the effect of isoproterenol on EHTs. n = 11.

B. Comparison of the duration and peak beating frequency of the effect of isoproterenol on EHTs. n = 11.

C. The contractile force after treatment with different concentrations of isoproterenol. n = 11.

D. The beating frequency after treatment with different concentrations of isoproterenol. n = 11.

3.7.3 High-frequency electrical stimulation

It has been proposed that increasing the intensity and frequency of electrical stimulation of the EHTs may promote tissue maturation and increase contractile force(87). The frequency of electrical stimulation of EHTs was therefore gradually increased at day 7 after culture in BMCCs. For control-EHTs, stimulation at higher frequencies damaged the EHTs to such extent that measurements were not possible. At a stimulation frequency of 3.0 Hz, capture was lost in some beats, suggesting that the refractory period was too long (Figure 27A), and that increasing the stimulation frequency even further would not result in higher contraction frequencies. For HRA-EHTs, contractile force after 72 hours of electrical stimulation at 1.5 and 3.0 Hz was higher as compared to stimulation at 1.0 Hz, with 3.0 Hz yielding higher contractile force as compared to 1.5 Hz (Figure 27B). Although there was a slight decrease in contractile force after switching to 1.0 Hz electrical stimulation, contractile force was still significantly higher than before applying electrical stimulation (Figure 27C).

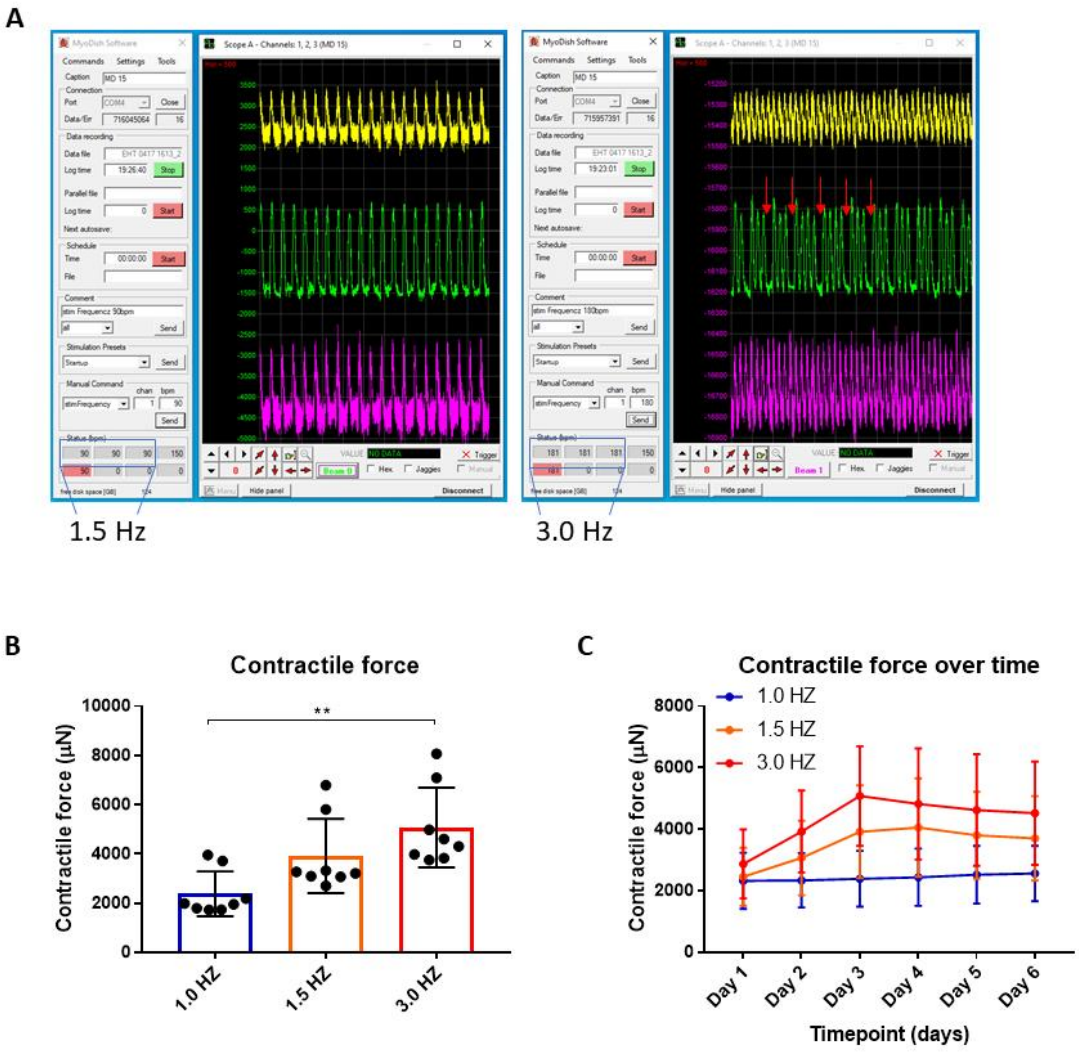

Figure 27. The response of EHTs to electrical stimulation.

A. The contraction waveform of EHTs under high-frequency electrical stimulation. The red arrow represents the refractory period of EHT.

B. The contractile force after different electrical stimulation frequencies. One-way ANOVA, Tukey's multiple comparison test. **$p < 0.01$.

C. The contractile force in different electrical stimulation groups over time. $n = 8$.

4. Discussion

In our study, reanalysis of existing single cell sequencing dataset of fetal hearts yielded the characteristics of CMs in 5 – 7 weeks old fetuses and identified the marker genes of LV and RV. As markers of LV and RV, TBX5, CORIN, NKX2.5, TBX20, and GATA4, that were confirmed in porcine and human myocardium, and subsequently used to classify hiPSC derived CMs as LV- or RV- like. We showed that addition of RA in a concentration of 0.1 µM (HRA group) resulted in a LV-like phenotype whereas absence of RA, or RA at a concentration of 0.05 µM (LRA group) resulted in a more RV-like phenotype. iPSCs-derived CMs were subsequently used to generate EHTs. HRA-EHTs showed higher expression of left ventricular marker genes, higher contractile force and increased sensitivity to β-adrenergic stimulation and hypoxia, whereas control- and LRA-EHTs showed higher expression of RV-marker genes. The implication of our findings will be further discussed below.

4.1 Marker genes of the LV and RV

In order to identify whether the differentiated cardiomyocytes were mainly left or right ventricular cardiomyocytes, we screened cardiomyocyte marker genes of the LV and RV according to previous literature. In the process of heart development, the LV develops from cardiac progenitor cells (CPCs) of the first FHF characterized by TBX5, NKX2.5(79, 88, 89) (Figure 28), while the RV, outflow tract, and some of the atria develop from the SHF's CPCs, which are identified by the gene ISL1(79, 90-92). With the maturation of precursor cells, those genes become markers for the subtype of cardiomyocytes with left or right ventricular phenotypes. Previous studies have shown that hiPSC-CM with high expression of TBX5 and NKX2.5 appears to be more genetically and functionally similar to CMs in the LV(36). At the same time, CORIN is one of the cell-surface markers that can be used to identify the TBX5+ and NKX2.5+ subpopulations(36) (Figure 29). Other studies have also provided conclusions about the marker genes of LV and RV. For instance, NKX2.5 designates the identity of the ventricular chamber, while TBX5 is one of the TFs involved in the development of the LV(93, 94). Connexin-43, TBX5 and IRX4 are the left ventricular specific proteins(95). Progenitors for the human RV are classified as posterior SHF, and TBX1+, ISL1+ precursor cells give rise to the right ventricle and outflow tract(14), which means TBX1

and ISL1 could be the marker genes of RV. For the studies in animals, Tbx5 expression was lacking in the right ventricle of mice and chickens(96). Tbx20 expression, which the left ventricle lacks, distinguishes the right ventricle in chicks(14, 93). In summary, based on the embryonic development of cardiac cells and a comparison of left and right ventricular marker genes, along with our comparative analysis in fetuses, adult humans, and swine, we can designate TBX5, NKX2.5, MEF2C, and CORIN as marker genes for left ventricular cardiomyocytes, while TBX20, ISL1 and GATA4 serve as marker genes for the right ventricle.

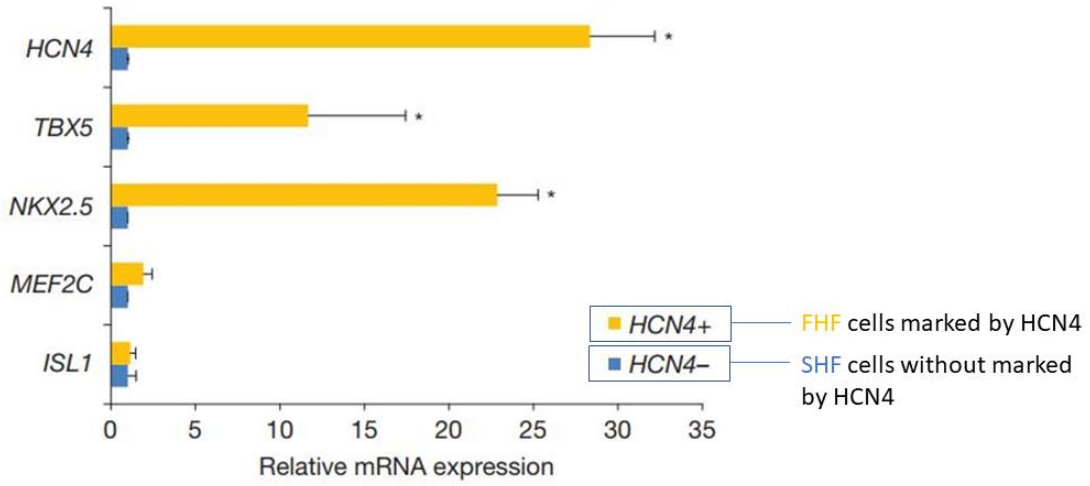

Figure 28. The expression levels of TBX5 and NKX2.5 are synchronized with the expression levels of FHF marker genes(79).

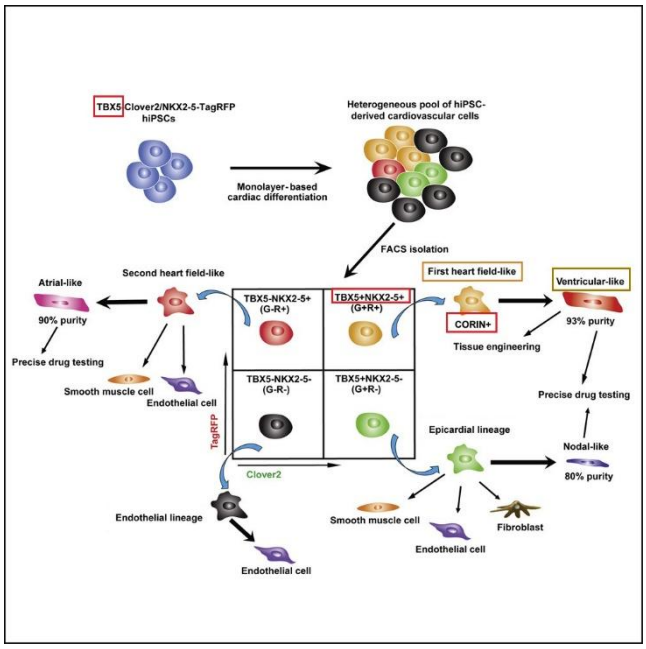

Figure 29. Schematic diagram of the expression of marker genes during the differentiation process of hiPSC(36).

The red box indicates that TBX5 and NKX2.5 can serve as marker genes for the first heart field (yellow box) and ventricular subpopulations (yellow box) during differentiation. The red box represents the marker genes of the left ventricle.

4.2 The relationship between RA signaling pathway and ventricular differentiation transcription factors

Our study focused on the differentiation of hiPSCs into left and right ventricular lineages, and we found that a precise concentration and timing of RA were necessary for left ventricular specification. The RA intervention phase aligned with the developmental stage of heart mesoderm cells and heart precursor cells in our study. Notably, the left ventricular marker genes, TBX5, NKX2.5, and CORIN, exhibited significantly increased expression in the HRA group after 20 days of differentiation. This discovery underscores the critical role of RA in driving hiPSC-CM differentiation towards a left ventricle-like phenotype. However, the precise mechanism through which RA signaling influences cardiac progenitor populations during hiPSC differentiation remains incompletely understood(97). RA, derived from vitamin A, acts as a lipophilic molecule and serves as a ligand for nuclear RA receptors (RARs)(98), converting them from transcriptional repressors to activators. RA's impact on development and cellular differentiation is mediated through retinoid receptors, which bind to specific DNA sequences called retinoic acid response elements (RAREs), thereby influencing the transcription of target genes(99).

Although the precise methodology through which RA guides hiPSC-CM differentiation toward a right ventricle-like phenotype remains unclear. Our RNA sequencing results identified that RA treatment affected expression of HOX genes in EHTs, which is consistent with observations that HOX genes feature RA-response elements (RAREs) in their enhancers or proximal promoters(82). As HOX genes have been shown to play a critical role during heart development(81), modulation of HOX may be a potential mechanism by which RA promotes hiPSC-CM differentiation. Furthermore, RA treatment was shown to upregulate expression of the transcription factors TBX5, NKX2.5 and MEF2C, while downregulating TBX20 and GATA4 in iPSC-CM as well as EHTs. These findings are consistent with their expression pattern in the LV and RV in the embryonic heart, and together with the specific ventricular

expression pattern of the RA receptors RARA and RARB, provide a mechanism through which CMs are directed towards an LV lineage.

4.3 EHT from the HRA group is phenotypically similar to LV

The use of primary human CMs derived from patients in *in vitro* studies poses challenges due to difficulties in their acquisition, preservation, and limited availability, which constrains their broader applicability and development in experimental research(100). EHT, a product of the marriage of biology and engineering, serves to summarize the extremely complex human physiology. It combines different matrices or scaffolds with different cell types to simulate multicellular heart tissue(101). The BMCC system used in our study to cultivate EHT is one of the most advanced myocardial biomimetic culture systems. It provided a stable growth environment, nutrient supply, and allowed us to assess EHT functionality by manipulating environmental parameters(102). The human LV and RV exhibit significant functional and structural differences. The LV has greater contractility, higher oxygen consumption, increased sensitivity to hypoxic environments and pressure loads, but weaker automaticity compared to the RV(103). In our study, EHTs from the HRA group displayed enhanced contractility, increased oxygen consumption. Without external electrical stimulation, the spontaneous beating frequency of the EHTs in the HRA group was comparatively lower, indicating a relatively weaker automaticity. Additionally, when subjected to chemical stimulation with isoprenaline, the HRA group displayed increased contractile force and beating frequency. These findings, coupled with the high expression of left ventricular marker genes in the HRA group, collectively indicate that the left ventricular characteristics of iPSC-CM persist during EHT development, thereby providing an *in vitro* model for the future study of the LV, particularly in disease modeling, drug screening, precision medicine, and potentially even regenerative medicine(104).

4.4 Extracellular matrix affects the contractile force of EHT

Our study shows that RA treatment modulates the contractile force of EHT by influencing the extracellular matrix, cell-cell junctions and intermediate filament proteins. Our sequencing and functional data underscore the importance of cellular structural components, cell-cell and cell-matrix connectivity for development of cardiac

force. One significant distinction between EHTs and CMs lies in the presence of a substantial cell population within EHT, complemented by the inclusion of an ECM that facilitates robust cell adhesion. Throughout the entire developmental continuum, spanning from the progenitor cell stage to ventricular differentiation and maturation, the ECM serves as a pivotal conduit for multiple signaling pathways, exerting profound influences on the standard progression of cardiac function and morphology(105, 106). In the context of the adult heart, the ECM network assumes an essential role in maintaining cardiac homeostasis, fulfilling its functions not only in structural reinforcement but also in facilitating force transmission, as well as mediating the transmission of critical signals to cardiomyocytes, vascular cells, and interstitial cells(107, 108). Alterations in the structural and biochemical composition of the ECM may exhibit a close association with the pathogenesis of heart failure characterized by reduced ejection fraction as well as heart failure with preserved ejection fraction(109). The nature of molecular and biochemical changes within the ECM during heart failure is contingent upon the specific type of damage incurred. Pressure overload initiates the early activation of the matrix synthesis program within cardiac fibroblasts, leading to myofibroblast transformation and concurrent stimulation of structural and stromal ECM protein synthesis(110).

Previous research has established that intermediate filament proteins can directly influence transcription of transcription factors such as NKX2.5, MEF2C thereby exerting an impact on myocardial regeneration and differentiation(111). Furthermore, EHTs derived from patients suffering from dilated cardiomyopathy showed that the absence of intermediate filament proteins resulted in myocardial tissue dilation, mitochondrial dysfunction, and diminished contractile capabilities(80).

The mRNA sequencing results and PPI network analysis suggest that PPARG may play a crucial role in regulating the extracellular matrix of EHT in the context of RA. Indeed, it has been demonstrated that PPARG is important for myocardium development and ventricular septation(84).

Our research results are in concordance with previous investigations(112, 113), emphasizing that the generation of contractile force by EHTs is governed not only by CMs contractile function, but also by CM-CM and CM- extracellular matrix-connections that may subsequently impact the expression and function of transcription factors. This viewpoint underscores the structural and functional resemblance between

EHTs and myocardial tissue, thereby aiding the development of *in vitro* experimental models and the progress of myocardial replacement therapy.

4.5 Electrical stimulation enhances EHT maturation

Electrical stimulation stands as a highly effective strategy for fostering the maturation of EHT in *in vitro* cultures. Numerous studies have demonstrated that both short-term and prolonged electrical stimulation can augment EHT's contractile force, enhance its Ca^{2+} handling capacity, and improve other electrophysiological attributes, with these enhancements proving to be enduring and irreversible(114-116). Across previous studies, the timing, frequency, and duration of electrical stimulation applications exhibit variations. The application of electrical stimulation during the early stages of hiPSC-CM differentiation can promote the emergence of more refined and mature CM phenotypes(115). When correspondence with short-term stimulation, continuous 4-week electrical stimulation also proves more efficacious in advancing the maturation of hiPSC-CM(117). Variations in electrical stimulation frequencies exert discernible impacts on the maturation of hiPSC-CM. The frequency of electrical stimulation can influence hiPSC-CM maturation, with research indicating that frequencies below 6 Hz are associated with stronger structures and more mature functions. Increasing the frequency from 1 Hz to 6 Hz, rather than 3 Hz, has been found to induce optimal maturation(118). However, research on frequencies above 6 Hz is limited, as they significantly exceed the physiological range. Gradually increasing the electrical stimulation frequency to attain the target frequency proves more conducive to EHT maturation compared to direct frequency escalation to the desired level(119). While certain studies have reached divergent conclusions(118), our research suggests that a gradual increase in stimulation frequency appears more advantageous in safeguarding EHT integrity and extending cultivation duration. Additionally, our investigations revealed that 3 Hz represents the upper limit for electrical stimulation frequency in our EHT, as frequencies exceeding this threshold result in a gradual extension of the absolute refractory period, and therefore stimulating at higher frequencies fails to effectively enhance EHT's contraction frequency. We endeavored to enhance EHT's oxygen supply by elevating the shaking frequency of BMCC, aiming to boost the contraction frequency at elevated stimulation frequencies; however, the outcomes proved unsatisfactory. Augmenting EHT's oxygen supply failed to enhance its contractile force, contractile frequency, and reduce the absolute refractory period.

However, our study identified that, in comparison to electric stimulation frequencies of 1.5 Hz and 1 Hz, a frequency of 3 Hz consistently enhances EHT's contractile force, which correspondence with previews study.

To summarize, electrical stimulation holds significant promise for generating functionally and structurally mature CMs, with applications ranging from disease modeling and drug screening to potential clinical use. Subsequent research endeavors may uncover more precise mechanisms governing the EHT's response to electrical stimulation. Concurrently, further investigations were warranted to determine the optimal amplitude, frequency, timing, and duration of electrical stimulation. Ultimately, despite electrical stimulation, a substantial disparity persists between adult heart tissue and cultured EHTs. Bridging this gap necessitates the development of a system that amalgamates diverse strategies for promoting maturation.

4.6 Clinicial implications

The continuous functioning of the heart, from early embryonic development to adulthood, is essential for the survival of all animals. Congenital and acquired heart diseases can have devastating effects, rendering to adult mortality(120). Most heart diseases result from cardiomyocyte loss, including conditions such as ischemic coronary artery disease and hypertension, which impair the heart's pumping capacity and ultimately lead to death(121). Furthermore, the hearts of adult mammals lack the capacity to efficiently generate new cardiomyocytes to repair damage. Although specific drugs and mechanical devices can temporarily improve heart function, they cannot replace the lost myocardial tissue and offer only temporary relief. This emphasizes the necessity for innovative strategies focused on heart repair. Thus, by reactivating embryonic pathways, it becomes conceivable to exploit the cellular processes and regulatory mechanisms necessary for heart growth and development to repair the injured adult heart(122). A complementary strategy for heart regeneration and repair can be pursued by promoting cardiomyocyte dedifferentiation and proliferation through the activation of mitotic signaling pathways associated with embryonic heart differentiation.

Owing to the analogous differentiation and proliferation capabilities of stem cells compared to embryonic cells, there has been a substantial surge of interest and investment in the advancement of stem cell-based cardiac repair therapies(123-125).

Studies have suggested that the direct injection of stem cells and other cell types into the damaged heart or coronary circulation results in modest enhancements in heart function in both animal models and humans(126, 127). However, the notion that transplanted cells survive within the damaged heart was inadequately supported by evidence, and the precise mechanism behind the observed cardiac improvement following stem cell delivery remained unclear. One possibility was that the paracrine signaling activity of the transplanted cells was accountable for the transient improvement observed following stem cell transplantation. To enhance heart regeneration and replace cardiomyocytes after cardiac injury and illness, additional innovative treatments are still needed(128).

While previous studies have achieved considerable success in cardiomyocyte differentiation, they frequently yielded heterogeneous populations of cardiovascular cells, encompassing ventricular-like, atrial, and pacemaker-like cells(39, 129, 130). Our study specifically concentrates on hiPSC differentiation into left ventricular lineages, and we have ascertained the requirement for a precise concentration of RA for left ventricular specification. Through the analysis of distinct gene expression patterns in the fetal LV and RV during development, supplemented by existing literature, we have successfully identified the marker genes specific to the LV. By using a precise concentration of RA as an intervention during a specific phase of the differentiation process, we have proficiently generated cardiomyocytes that possess functional and genetic traits akin to those of the fetal LV. Considering the timing of fetal heartbeats and the onset of contractions in our differentiated cardiomyocytes, we hypothesize that our hiPSC-CM aligns with the developmental stage of the fetus during 5 - 7 weeks.

While our differentiated hiPSC-CMs may still include non-LV-like CMs, it undeniably establishes the groundwork for the subsequent purification of cardiomyocyte subtypes. Consequently, the cardiomyocytes and engineered heart tissues (EHTs) obtained in our study have the potential to address several of the aforementioned challenges. Firstly, the cardiomyocyte seed cells we utilized were derived from adult cells, alleviating ethical constraints. Secondly, we have improved the differentiation process by leveraging established, mature differentiation technologies, leading to increased maturity and purity in cardiomyocytes. Thirdly, we have effectively integrated cell fusion into cardiomyoid tissue, laying the groundwork for potential tissue transplantation in the future. Last but not least, our research offers a robust *in vitro* model for studying left ventricular function and developing novel medications.

4.7 Research limitations

Despite utilizing the proper concentration of RA to stimulate hiPSC differentiation into CM and EHT with a left ventricle-like phenotype, our study has some limitations. First, the exact mechanisms by which the RA guides hiPSC-CM differentiation towards RV-like cardiomyocytes remain to be determined. Secondly, the regulatory mechanism through which RA modulates the expression of genes and proteins associated with the extracellular matrix in EHT remains incompletely understood. The mRNA sequencing results and PPI network analysis suggest that the PPARG gene may play a crucial role in regulating the extracellular matrix of EHT in the context of RA. Along with this it has been demonstrated that PPARG is important for myocardium development and ventricular septation(84). Further investigation and validation are warranted. Thirdly, beside the TFs, microRNA (miR-1, miR-133, miR-208 and miR-499) have also been shown to be involved in embryonic heart development and cardiomyocyte identification(122). Further analysis of microRNA expression differences among different groups may provide more solid evidence to support our conclusion. Moving forward, our future investigations will aim to delve into the differentiation pathways leading to left and right ventricular, as well as atrial, CMs, with a focus on understanding the role of RA and potential interactions with other signaling pathways influencing differentiation.

5. Conclusion

The functional and genetic analysis of CM and EHT has provided valuable insights in our study. Specifically, the HRA group exhibited significantly elevated expression levels of CM maturation markers, as well as left ventricular markers, while the LRA and control groups showed pronounced expression of right ventricular markers. Moreover, the EHT derived from the HRA group demonstrated the highest contractility. These compelling findings strongly suggest that a 0.1 mM concentration of RA can effectively facilitate the differentiation of hiPSCs into CMs closely resembling the left ventricular phenotype. The RA signaling pathway exerts intricate control over pivotal transcription factors that play a fundamental role in CM development, likely serving as the molecular mechanism behind RA's facilitation of hiPSC differentiation into left ventricular CMs. Concurrently, our study substantiated the indispensable role of the extracellular matrix in augmenting the contractile force of engineered heart tissue (EHT). These collective findings not only deepen our comprehension of cardiac differentiation but also establish a foundation for future investigations into *in vitro* left ventricular function, personalized drug screening, and the advancement of precision medicine.

References

1. Maherali N, Ahfeldt T, Rigamonti A, Utikal J, Cowan C, Hochedlinger K. A high-efficiency system for the generation and study of human induced pluripotent stem cells. Cell Stem Cell. 2008;3(3):340-5.
2. Jiang Y, Zhang LL, Zhang F, Bi W, Zhang P, Yu XJ, et al. Dual human iPSC-derived cardiac lineage cell-seeding extracellular matrix patches promote regeneration and long-term repair of infarcted hearts. Bioact Mater. 2023;28:206-26.
3. Kobold S, Bultjer N, Stacey G, Mueller SC, Kurtz A, Mah N. History and current status of clinical studies using human pluripotent stem cells. Stem Cell Reports. 2023.
4. Repina NA, Johnson HJ, Bao X, Zimmermann JA, Joy DA, Bi SZ, et al. Optogenetic control of Wnt signaling models cell-intrinsic embryogenic patterning using 2D human pluripotent stem cell culture. Development. 2023.
5. Groeger M, Matsuo K, Heidary Arash E, Pereira A, Le Guillou D, Pino C, et al. Modeling and therapeutic targeting of inflammation-induced hepatic insulin resistance using human iPSC-derived hepatocytes and macrophages. Nat Commun. 2023;14(1):3902.
6. Ma J, Wang NY, Jagani R, Wang HS. Proarrhythmic toxicity of low dose bisphenol A and its analogs in human iPSC-derived cardiomyocytes and human cardiac organoids through delay of cardiac repolarization. Chemosphere. 2023;328:138562.
7. Kishino Y, Tohyama S, Morita Y, Soma Y, Tani H, Okada M, et al. Cardiac Regenerative Therapy Using Human Pluripotent Stem Cells for Heart Failure: A State-of-the-Art Review. J Card Fail. 2023;29(4):503-13.
8. Kobold S, Guhr A, Mah N, Bultjer N, Seltmann S, Seiler Wulczyn AEM, et al. A Manually Curated Database on Clinical Studies Involving Cell Products Derived from Human Pluripotent Stem Cells. Stem Cell Reports. 2020;15(2):546-55.
9. Burridge PW, Keller G, Gold JD, Wu JC. Production of de novo cardiomyocytes: human pluripotent stem cell differentiation and direct reprogramming. Cell Stem Cell. 2012;10(1):16-28.
10. Devine WP, Wythe JD, George M, Koshiba-Takeuchi K, Bruneau BG. Early patterning and specification of cardiac progenitors in gastrulating mesoderm. Elife. 2014;3.
11. Costello I, Pimeisl IM, Dräger S, Bikoff EK, Robertson EJ, Arnold SJ. The T-box transcription factor Eomesodermin acts upstream of Mesp1 to specify cardiac mesoderm during mouse gastrulation. Nat Cell Biol. 2011;13(9):1084-91.
12. Kuo CT, Morrisey EE, Anandappa R, Sigrist K, Lu MM, Parmacek MS, et al. GATA4 transcription factor is required for ventral morphogenesis and heart tube formation. Genes Dev. 1997;11(8):1048-60.
13. Waldo KL, Kumiski DH, Wallis KT, Stadt HA, Hutson MR, Platt DH, et al. Conotruncal myocardium arises from a secondary heart field. Development. 2001;128(16):3179-88.
14. Paige SL, Plonowska K, Xu A, Wu SM. Molecular regulation of cardiomyocyte differentiation. Circ Res. 2015;116(2):341-53.
15. Bruneau BG. The developmental genetics of congenital heart disease. Nature. 2008;451(7181):943-8.
16. Moorman AF, Christoffels VM. Cardiac chamber formation: development, genes, and evolution. Physiol Rev. 2003;83(4):1223-67.
17. Cho CH, Kim SS, Jeong MJ, Lee CO, Shin HS. The Na+ -Ca2+ exchanger is essential for embryonic heart development in mice. Mol Cells. 2000;10(6):712-22.
18. Schultheiss TM, Burch JB, Lassar AB. A role for bone morphogenetic proteins in the induction of cardiac myogenesis. Genes Dev. 1997;11(4):451-62.
19. Andrée B, Duprez D, Vorbusch B, Arnold HH, Brand T. BMP-2 induces ectopic expression of cardiac lineage markers and interferes with somite formation in chicken embryos. Mech Dev. 1998;70(1-2):119-31.
20. Pandur P, Läsche M, Eisenberg LM, Kühl M. Wnt-11 activation of a non-canonical Wnt signalling pathway is required for cardiogenesis. Nature. 2002;418(6898):636-41.
21. Pinton L, Khedr M, Lionello VM, Sarcar S, Maffioletti SM, Dastidar S, et al. 3D human induced pluripotent stem cell-derived bioengineered skeletal muscles for tissue, disease and therapy modeling. Nat Protoc. 2023;18(4):1337-76.

22. Akbarzadeh A, Sobhani S, Soltani Khaboushan A, Kajbafzadeh AM. Whole-Heart Tissue Engineering and Cardiac Patches: Challenges and Promises. Bioengineering (Basel). 2023;10(1).
23. Guo R, Morimatsu M, Feng T, Lan F, Chang D, Wan F, et al. Stem cell-derived cell sheet transplantation for heart tissue repair in myocardial infarction. Stem Cell Res Ther. 2020;11(1):19.
24. Tani H, Kobayashi E, Yagi S, Tanaka K, Kameda-Haga K, Shibata S, et al. Heart-derived collagen promotes maturation of engineered heart tissue. Biomaterials. 2023;299:122174.
25. Querdel E, Reinsch M, Castro L, Köse D, Bähr A, Reich S, et al. Human Engineered Heart Tissue Patches Remuscularize the Injured Heart in a Dose-Dependent Manner. Circulation. 2021;143(20):1991-2006.
26. Miyamoto M, Nam L, Kannan S, Kwon C. Heart organoids and tissue models for modeling development and disease. Semin Cell Dev Biol. 2021;118:119-28.
27. Pecha S, Eschenhagen T, Reichenspurner H. Myocardial tissue engineering for cardiac repair. J Heart Lung Transplant. 2016;35(3):294-8.
28. Jiang Y, Park P, Hong SM, Ban K. Maturation of Cardiomyocytes Derived from Human Pluripotent Stem Cells: Current Strategies and Limitations. Mol Cells. 2018;41(7):613-21.
29. Scuderi GJ, Butcher J. Naturally Engineered Maturation of Cardiomyocytes. Front Cell Dev Biol. 2017;5:50.
30. Liu Y, Bai H, Guo F, Thai PN, Luo X, Zhang P, et al. PGC-1α activator ZLN005 promotes maturation of cardiomyocytes derived from human embryonic stem cells. Aging (Albany NY). 2020;12(8):7411-30.
31. Miki K, Deguchi K, Nakanishi-Koakutsu M, Lucena-Cacace A, Kondo S, Fujiwara Y, et al. ERRγ enhances cardiac maturation with T-tubule formation in human iPSC-derived cardiomyocytes. Nat Commun. 2021;12(1):3596.
32. Giacomelli E, Meraviglia V, Campostrini G, Cochrane A, Cao X, van Helden RWJ, et al. Human-iPSC-Derived Cardiac Stromal Cells Enhance Maturation in 3D Cardiac Microtissues and Reveal Non-cardiomyocyte Contributions to Heart Disease. Cell Stem Cell. 2020;26(6):862-79.e11.
33. Mannhardt I, Breckwoldt K, Letuffe-Brenière D, Schaaf S, Schulz H, Neuber C, et al. Human Engineered Heart Tissue: Analysis of Contractile Force. Stem Cell Reports. 2016;7(1):29-42.
34. Thavandiran N, Nunes SS, Xiao Y, Radisic M. Topological and electrical control of cardiac differentiation and assembly. Stem Cell Res Ther. 2013;4(1):14.
35. Lu K, Seidel T, Cao-Ehlker X, Dorn T, Batcha AMN, Schneider CM, et al. Progressive stretch enhances growth and maturation of 3D stem-cell-derived myocardium. Theranostics. 2021;11(13):6138-53.
36. Zhang JZ, Termglinchan V, Shao NY, Itzhaki I, Liu C, Ma N, et al. A Human iPSC Double-Reporter System Enables Purification of Cardiac Lineage Subpopulations with Distinct Function and Drug Response Profiles. Cell Stem Cell. 2019;24(5):802-11.e5.
37. Lee JH, Protze SI, Laksman Z, Backx PH, Keller GM. Human Pluripotent Stem Cell-Derived Atrial and Ventricular Cardiomyocytes Develop from Distinct Mesoderm Populations. Cell Stem Cell. 2017;21(2):179-94.e4.
38. Lemme M, Ulmer BM, Lemoine MD, Zech ATL, Flenner F, Ravens U, et al. Atrial-like Engineered Heart Tissue: An In Vitro Model of the Human Atrium. Stem Cell Reports. 2018;11(6):1378-90.
39. Cyganek L, Tiburcy M, Sekeres K, Gerstenberg K, Bohnenberger H, Lenz C, et al. Deep phenotyping of human induced pluripotent stem cell-derived atrial and ventricular cardiomyocytes. JCI Insight. 2018;3(12).
40. Birket MJ, Ribeiro MC, Verkerk AO, Ward D, Leitoguinho AR, den Hartogh SC, et al. Expansion and patterning of cardiovascular progenitors derived from human pluripotent stem cells. Nat Biotechnol. 2015;33(9):970-9.
41. Protze SI, Liu J, Nussinovitch U, Ohana L, Backx PH, Gepstein L, et al. Sinoatrial node cardiomyocytes derived from human pluripotent cells function as a biological pacemaker. Nat Biotechnol. 2017;35(1):56-68.
42. Guadix JA, Orlova VV, Giacomelli E, Bellin M, Ribeiro MC, Mummery CL, et al. Human Pluripotent Stem Cell Differentiation into Functional Epicardial Progenitor Cells. Stem Cell Reports. 2017;9(6):1754-64.
43. Meier AB, Zawada D, De Angelis MT, Martens LD, Santamaria G, Zengerle S, et al. Epicardioid single-cell genomics uncovers principles of human epicardium biology in heart development and disease. Nat Biotechnol. 2023.
44. Duester G. Retinoic acid synthesis and signaling during early organogenesis. Cell. 2008;134(6):921-31.

45. Ghyselinck NB, Duester G. Retinoic acid signaling pathways. Development. 2019;146(13).
46. Wiesinger A, Boink GJJ, Christoffels VM, Devalla HD. Retinoic acid signaling in heart development: Application in the differentiation of cardiovascular lineages from human pluripotent stem cells. Stem Cell Reports. 2021;16(11):2589-606.
47. Hofbauer P, Jahnel SM, Papai N, Giesshammer M, Deyett A, Schmidt C, et al. Cardioids reveal self-organizing principles of human cardiogenesis. Cell. 2021;184(12):3299-317.e22.
48. Tan JJ, Guyette JP, Miki K, Xiao L, Kaur G, Wu T, et al. Human iPS-derived pre-epicardial cells direct cardiomyocyte aggregation expansion and organization in vitro. Nat Commun. 2021;12(1):4997.
49. Ivanovitch K, Soro-Barrio P, Chakravarty P, Jones RA, Bell DM, Mousavy Gharavy SN, et al. Ventricular, atrial, and outflow tract heart progenitors arise from spatially and molecularly distinct regions of the primitive streak. PLoS Biol. 2021;19(5):e3001200.
50. Devalla HD, Schwach V, Ford JW, Milnes JT, El-Haou S, Jackson C, et al. Atrial-like cardiomyocytes from human pluripotent stem cells are a robust preclinical model for assessing atrial-selective pharmacology. EMBO Mol Med. 2015;7(4):394-410.
51. Miao S, Zhao D, Wang X, Ni X, Fang X, Yu M, et al. Retinoic acid promotes metabolic maturation of human Embryonic Stem Cell-derived Cardiomyocytes. Theranostics. 2020;10(21):9686-701.
52. Lescroart F, Wang X, Lin X, Swedlund B, Gargouri S, Sànchez-Dànes A, et al. Defining the earliest step of cardiovascular lineage segregation by single-cell RNA-seq. Science. 2018;359(6380):1177-81.
53. Feneck E, Logan M. The Role of Retinoic Acid in Establishing the Early Limb Bud. Biomolecules. 2020;10(2).
54. Yin L, Wang FY, Zhang W, Wang X, Tang YH, Wang T, et al. RA signaling pathway combined with Wnt signaling pathway regulates human-induced pluripotent stem cells (hiPSCs) differentiation to sinus node-like cells. Stem Cell Res Ther. 2022;13(1):324.
55. Hiroi Y, Kudoh S, Monzen K, Ikeda Y, Yazaki Y, Nagai R, et al. Tbx5 associates with Nkx2-5 and synergistically promotes cardiomyocyte differentiation. Nat Genet. 2001;28(3):276-80.
56. Bruneau BG, Nemer G, Schmitt JP, Charron F, Robitaille L, Caron S, et al. A murine model of Holt-Oram syndrome defines roles of the T-box transcription factor Tbx5 in cardiogenesis and disease. Cell. 2001;106(6):709-21.
57. Linhares VL, Almeida NA, Menezes DC, Elliott DA, Lai D, Beyer EC, et al. Transcriptional regulation of the murine Connexin40 promoter by cardiac factors Nkx2-5, GATA4 and Tbx5. Cardiovasc Res. 2004;64(3):402-11.
58. Bruneau BG. Signaling and transcriptional networks in heart development and regeneration. Cold Spring Harb Perspect Biol. 2013;5(3):a008292.
59. McCulley DJ, Black BL. Transcription factor pathways and congenital heart disease. Curr Top Dev Biol. 2012;100:253-77.
60. Waardenberg AJ, Ramialison M, Bouveret R, Harvey RP. Genetic networks governing heart development. Cold Spring Harb Perspect Med. 2014;4(11):a013839.
61. Targoff KL, Colombo S, George V, Schell T, Kim SH, Solnica-Krezel L, et al. Nkx genes are essential for maintenance of ventricular identity. Development. 2013;140(20):4203-13.
62. Lin Q, Schwarz J, Bucana C, Olson EN. Control of mouse cardiac morphogenesis and myogenesis by transcription factor MEF2C. Science. 1997;276(5317):1404-7.
63. Bruneau BG, Bao ZZ, Fatkin D, Xavier-Neto J, Georgakopoulos D, Maguire CT, et al. Cardiomyopathy in Irx4-deficient mice is preceded by abnormal ventricular gene expression. Mol Cell Biol. 2001;21(5):1730-6.
64. Chen HX, Zhang X, Hou HT, Wang J, Yang Q, Wang XL, et al. Identification of a novel and functional mutation in the TBX5 gene in a patient by screening from 354 patients with isolated ventricular septal defect. Eur J Med Genet. 2017;60(7):385-90.
65. Zhang Y, Sun YM, Xu YJ, Zhao CM, Yuan F, Guo XJ, et al. A New TBX5 Loss-of-Function Mutation Contributes to Congenital Heart Defect and Atrioventricular Block. Int Heart J. 2020;61(4):761-8.
66. Cui Y, Zheng Y, Liu X, Yan L, Fan X, Yong J, et al. Single-Cell Transcriptome Analysis Maps the Developmental Track of the Human Heart. Cell reports. 2019;26(7):1934-50.e5.
67. Fischer C, Milting H, Fein E, Reiser E, Lu K, Seidel T, et al. Long-term functional and structural preservation of precision-cut human myocardium under continuous electromechanical stimulation in vitro. Nat Commun. 2019;10(1):117.
68. Sen P, Shashikadze B, Flenkenthaler F, Van de Kamp E, Tian S, Meng C, et al. Proteomics- and Metabolomics-Based Analysis of Metabolic Changes in a Swine Model of Pulmonary Hypertension. Int J Mol Sci. 2023;24(5).

69. Moretti A, Laugwitz KL, Dorn T, Sinnecker D, Mummery C. Pluripotent stem cell models of human heart disease. Cold Spring Harb Perspect Med. 2013;3(11).
70. Chen G, Gulbranson DR, Hou Z, Bolin JM, Ruotti V, Probasco MD, et al. Chemically defined conditions for human iPSC derivation and culture. Nat Methods. 2011;8(5):424-9.
71. Cashman TJ, Josowitz R, Gelb BD, Li RA, Dubois NC, Costa KD. Construction of Defined Human Engineered Cardiac Tissues to Study Mechanisms of Cardiac Cell Therapy. J Vis Exp. 2016(109):e53447.
72. Tiburcy M, Hudson JE, Balfanz P, Schlick S, Meyer T, Chang Liao ML, et al. Defined Engineered Human Myocardium With Advanced Maturation for Applications in Heart Failure Modeling and Repair. Circulation. 2017;135(19):1832-47.
73. Liao Y, Smyth GK, Shi W. featureCounts: an efficient general purpose program for assigning sequence reads to genomic features. Bioinformatics. 2014;30(7):923-30.
74. Anders S, Huber W. Differential expression analysis for sequence count data. Genome Biol. 2010;11(10):R106.
75. Young MD, Wakefield MJ, Smyth GK, Oshlack A. Gene ontology analysis for RNA-seq: accounting for selection bias. Genome Biol. 2010;11(2):R14.
76. Klattenhoff CA, Scheuermann JC, Surface LE, Bradley RK, Fields PA, Steinhauser ML, et al. Braveheart, a long noncoding RNA required for cardiovascular lineage commitment. Cell. 2013;152(3):570-83.
77. Lozano-Velasco E, Garcia-Padilla C, Del Mar Muñoz-Gallardo M, Martinez-Amaro FJ, Caño-Carrillo S, Castillo-Casas JM, et al. Post-Transcriptional Regulation of Molecular Determinants during Cardiogenesis. Int J Mol Sci. 2022;23(5).
78. Cornwell JD, McDermott JC. MEF2 in cardiac hypertrophy in response to hypertension. Trends Cardiovasc Med. 2023;33(4):204-12.
79. Später D, Abramczuk MK, Buac K, Zangi L, Stachel MW, Clarke J, et al. A HCN4+ cardiomyogenic progenitor derived from the first heart field and human pluripotent stem cells. Nat Cell Biol. 2013;15(9):1098-106.
80. Vermeer MC, Bolling MC, Bliley JM, Arevalo Gomez KF, Pavez-Giani MG, Kramer D, et al. Gain-of-function mutation in ubiquitin-ligase KLHL24 causes desmin degradation and dilatation in hiPSC-derived engineered heart tissues. J Clin Invest. 2021;131(17).
81. Roux M, Zaffran S. Hox Genes in Cardiovascular Development and Diseases. J Dev Biol. 2016;4(2).
82. Alexander T, Nolte C, Krumlauf R. Hox genes and segmentation of the hindbrain and axial skeleton. Annu Rev Cell Dev Biol. 2009;25:431-56.
83. Panebianco C, Oben JA, Vinciguerra M, Pazienza V. Senescence in hepatic stellate cells as a mechanism of liver fibrosis reversal: a putative synergy between retinoic acid and PPAR-gamma signalings. Clin Exp Med. 2017;17(3):269-80.
84. Zhou L, Wang ZZ, Xiao ZC, Tu L. Effects of PPAR-γ in the Myocardium on the Development of Ventricular Septation. Curr Med Sci. 2020;40(2):313-9.
85. Sabourin J, Beauvais A, Luo R, Montani D, Benitah JP, Masson B, et al. The SOCE Machinery: An Unbalanced Knowledge between Left and Right Ventricular Pathophysiology. Cells. 2022;11(20).
86. Andersen S, Andersen A, de Man FS, Nielsen-Kudsk JE. Sympathetic nervous system activation and β-adrenoceptor blockade in right heart failure. Eur J Heart Fail. 2015;17(4):358-66.
87. Ronaldson-Bouchard K, Yeager K, Teles D, Chen T, Ma S, Song L, et al. Engineering of human cardiac muscle electromechanically matured to an adult-like phenotype. Nat Protoc. 2019;14(10):2781-817.
88. Buckingham M, Meilhac S, Zaffran S. Building the mammalian heart from two sources of myocardial cells. Nat Rev Genet. 2005;6(11):826-35.
89. Pezhouman A, Engel JL, Nguyen NB, Skelton RJP, Gilmore WB, Qiao R, et al. Isolation and characterization of human embryonic stem cell-derived heart field-specific cardiomyocytes unravels new insights into their transcriptional and electrophysiological profiles. Cardiovasc Res. 2022;118(3):828-43.
90. Vincent SD, Buckingham ME. How to make a heart: the origin and regulation of cardiac progenitor cells. Curr Top Dev Biol. 2010;90:1-41.
91. Laugwitz KL, Moretti A, Caron L, Nakano A, Chien KR. Islet1 cardiovascular progenitors: a single source for heart lineages? Development. 2008;135(2):193-205.
92. Martin-Puig S, Wang Z, Chien KR. Lives of a heart cell: tracing the origins of cardiac progenitors. Cell Stem Cell. 2008;2(4):320-31.

93. Takeuchi JK, Ohgi M, Koshiba-Takeuchi K, Shiratori H, Sakaki I, Ogura K, et al. Tbx5 specifies the left/right ventricles and ventricular septum position during cardiogenesis. Development. 2003;130(24):5953-64.
94. Plageman TF, Jr., Yutzey KE. Differential expression and function of Tbx5 and Tbx20 in cardiac development. J Biol Chem. 2004;279(18):19026-34.
95. Satthenapalli R, Lee S, Bellae Papannarao J, Hore TA, Chakraborty A, Jones PP, et al. Stage-specific regulation of signalling pathways to differentiate pluripotent stem cells to cardiomyocytes with ventricular lineage. Stem Cell Res Ther. 2022;13(1):185.
96. Bruneau BG, Logan M, Davis N, Levi T, Tabin CJ, Seidman JG, et al. Chamber-specific cardiac expression of Tbx5 and heart defects in Holt-Oram syndrome. Dev Biol. 1999;211(1):100-8.
97. Duong TB, Holowiecki A, Waxman JS. Retinoic acid signaling restricts the size of the first heart field within the anterior lateral plate mesoderm. Dev Biol. 2021;473:119-29.
98. Rhinn M, Dollé P. Retinoic acid signalling during development. Development. 2012;139(5):843-58.
99. Wobus AM, Kaomei G, Shan J, Wellner MC, Rohwedel J, Ji G, et al. Retinoic acid accelerates embryonic stem cell-derived cardiac differentiation and enhances development of ventricular cardiomyocytes. J Mol Cell Cardiol. 1997;29(6):1525-39.
100. Voigt N, Pearman CM, Dobrev D, Dibb KM. Methods for isolating atrial cells from large mammals and humans. J Mol Cell Cardiol. 2015;86:187-98.
101. Owen TJ, Harding SE. Multi-cellularity in cardiac tissue engineering, how close are we to native heart tissue? J Muscle Res Cell Motil. 2019;40(2):151-7.
102. Waleczek FJG, Sansonetti M, Xiao K, Jung M, Mitzka S, Dendorfer A, et al. Chemical and mechanical activation of resident cardiac macrophages in the living myocardial slice ex vivo model. Basic Res Cardiol. 2022;117(1):63.
103. Petersen SE, Jensen B, Aung N, Friedrich MG, McMahon CJ, Mohiddin SA, et al. Excessive Trabeculation of the Left Ventricle: JACC: Cardiovascular Imaging Expert Panel Paper. JACC Cardiovasc Imaging. 2023;16(3):408-25.
104. Sacchetto C, Vitiello L, de Windt LJ, Rampazzo A, Calore M. Modeling Cardiovascular Diseases with hiPSC-Derived Cardiomyocytes in 2D and 3D Cultures. Int J Mol Sci. 2020;21(9).
105. Alfano D, Altomonte A, Cortes C, Bilio M, Kelly RG, Baldini A. Tbx1 regulates extracellular matrix-cell interactions in the second heart field. Hum Mol Genet. 2019;28(14):2295-308.
106. Rowton M, Guzzetta A, Rydeen AB, Moskowitz IP. Control of cardiomyocyte differentiation timing by intercellular signaling pathways. Semin Cell Dev Biol. 2021;118:94-106.
107. Bonnans C, Chou J, Werb Z. Remodelling the extracellular matrix in development and disease. Nat Rev Mol Cell Biol. 2014;15(12):786-801.
108. Theocharis AD, Skandalis SS, Gialeli C, Karamanos NK. Extracellular matrix structure. Adv Drug Deliv Rev. 2016;97:4-27.
109. Iwanaga Y, Aoyama T, Kihara Y, Onozawa Y, Yoneda T, Sasayama S. Excessive activation of matrix metalloproteinases coincides with left ventricular remodeling during transition from hypertrophy to heart failure in hypertensive rats. J Am Coll Cardiol. 2002;39(8):1384-91.
110. Frangogiannis NG. The Extracellular Matrix in Ischemic and Nonischemic Heart Failure. Circ Res. 2019;125(1):117-46.
111. Nikouli S, Tsikitis M, Raftopoulou C, Gagos S, Psarras S, Capetanaki Y. Desmin deficiency affects the microenvironment of the cardiac side population and Sca1(+) stem cell population of the adult heart and impairs their cardiomyogenic commitment. Cell Tissue Res. 2022;389(2):309-26.
112. Gentile A, Bensimon-Brito A, Priya R, Maischein HM, Piesker J, Guenther S, et al. The EMT transcription factor Snai1 maintains myocardial wall integrity by repressing intermediate filament gene expression. Elife. 2021;10.
113. Tsikitis M, Galata Z, Mavroidis M, Psarras S, Capetanaki Y. Intermediate filaments in cardiomyopathy. Biophys Rev. 2018;10(4):1007-31.
114. Shen S, Sewanan LR, Shao S, Halder SS, Stankey P, Li X, et al. Physiological calcium combined with electrical pacing accelerates maturation of human engineered heart tissue. Stem Cell Reports. 2022;17(9):2037-49.
115. Crestani T, Steichen C, Neri E, Rodrigues M, Fonseca-Alaniz MH, Ormrod B, et al. Electrical stimulation applied during differentiation drives the hiPSC-CMs towards a mature cardiac conduction-like cells. Biochem Biophys Res Commun. 2020;533(3):376-82.

116. Nunes SS, Miklas JW, Liu J, Aschar-Sobbi R, Xiao Y, Zhang B, et al. Biowire: a platform for maturation of human pluripotent stem cell-derived cardiomyocytes. Nat Methods. 2013;10(8):781-7.
117. Hirt MN, Boeddinghaus J, Mitchell A, Schaaf S, Börnchen C, Müller C, et al. Functional improvement and maturation of rat and human engineered heart tissue by chronic electrical stimulation. J Mol Cell Cardiol. 2014;74:151-61.
118. Zhao Y, Rafatian N, Wang EY, Feric NT, Lai BFL, Knee-Walden EJ, et al. Engineering microenvironment for human cardiac tissue assembly in heart-on-a-chip platform. Matrix Biol. 2020;85-86:189-204.
119. Hong Y, Zhao Y, Li H, Yang Y, Chen M, Wang X, et al. Engineering the maturation of stem cell-derived cardiomyocytes. Front Bioeng Biotechnol. 2023;11:1155052.
120. Lopez AD, Mathers CD, Ezzati M, Jamison DT, Murray CJ. Global and regional burden of disease and risk factors, 2001: systematic analysis of population health data. Lancet. 2006;367(9524):1747-57.
121. Hill JA, Olson EN. Cardiac plasticity. N Engl J Med. 2008;358(13):1370-80.
122. Xin M, Olson EN, Bassel-Duby R. Mending broken hearts: cardiac development as a basis for adult heart regeneration and repair. Nat Rev Mol Cell Biol. 2013;14(8):529-41.
123. Segers VF, Lee RT. Stem-cell therapy for cardiac disease. Nature. 2008;451(7181):937-42.
124. Laflamme MA, Murry CE. Heart regeneration. Nature. 2011;473(7347):326-35.
125. Wollert KC, Drexler H. Cell therapy for the treatment of coronary heart disease: a critical appraisal. Nat Rev Cardiol. 2010;7(4):204-15.
126. Passier R, van Laake LW, Mummery CL. Stem-cell-based therapy and lessons from the heart. Nature. 2008;453(7193):322-9.
127. Ptaszek LM, Mansour M, Ruskin JN, Chien KR. Towards regenerative therapy for cardiac disease. Lancet. 2012;379(9819):933-42.
128. Mercola M, Ruiz-Lozano P, Schneider MD. Cardiac muscle regeneration: lessons from development. Genes Dev. 2011;25(4):299-309.
129. Blazeski A, Zhu R, Hunter DW, Weinberg SH, Zambidis ET, Tung L. Cardiomyocytes derived from human induced pluripotent stem cells as models for normal and diseased cardiac electrophysiology and contractility. Prog Biophys Mol Biol. 2012;110(2-3):166-77.
130. Friedman CE, Nguyen Q, Lukowski SW, Helfer A, Chiu HS, Miklas J, et al. Single-Cell Transcriptomic Analysis of Cardiac Differentiation from Human PSCs Reveals HOPX-Dependent Cardiomyocyte Maturation. Cell Stem Cell. 2018;23(4):586-98.e8.

Acknowledgments

I am deeply grateful to several individuals who played pivotal roles in my doctoral journey.

First and foremost, I extend my deepest gratitude to my supervisor, Prof. Dr. Daphne Merkus, for her friendliness, approachability, and academic rigor. When I initially arrived in Germany with limited English proficiency and experimental skills, she provided me a lot of encouragement. Her dedicated guidance throughout my academic journey has been invaluable, and I may not have successfully completed my studies without her. I am genuinely grateful for her unwavering support.

I extend my heartfelt appreciation to my co-supervisor, Prof. Dr. Andreas Dendorfer, for his invaluable guidance and support throughout my research journey. His patient and diligent assistance in overcoming various technical challenges during my experiments was instrumental to the success of this project.

I am also deeply grateful to Prof. Dr. Alessandra Moretti for generously providing me with iPSCs and sharing her expertise in cell culture techniques, which significantly contributed to the success of this study.

I am also deeply grateful to my co-supervisor PD. Dr. med. Sebastian Clauss for his guidance and insightful suggestions regarding my project.

I am indebted to Dr. Payel Sen for her tireless guidance throughout the experimental process, assisting me with every step.

I vividly recall my first day in our lab when Prof. Dr. Daphne Merkus introduced me to each team member. On that day, Dr. Payel Sen arranged my workspace, Jules Hamers familiarized me with the operating room, Theresa Sittig guided me to the restaurant, Brent Woestenburg instructed me in cell cultivation, and a few weeks later, Chiara d' Alessio assisted me with liquid nitrogen replenishment. Despite my limited English skills and challenges adapting to different cultures in my daily work and life, every team member showed care and respect towards me. I am fortunate to have been a part of an international team, where each member has displayed enthusiasm, friendliness, and unity through actions. I have made significant progress in various aspects, thanks to the support of every team member. I extend my heartfelt thanks to each and every one of them.

I also express my gratitude to my friend Zhengwu Sun, Kun Lu and the exceptional lab technician Claudia Fahney for their support in both experimental work and daily life.

I am deeply grateful to my colleagues and leaders in China, Prof. Dr. Pingshuan Dong, Prof. Dr. Shegan Gao, Prof. Dr. Xvming Yang, Prof. Jianxue Lian, and Prof. Zhengshun Xv, for their encouragement and support during my work in China and their substantial assistance during the CSC scholarship application process.

Last but certainly not least, I wish to express my heartfelt gratitude to my dear wife, Pei Zhang, for looking after our two children and our home while I pursued my studies. I am also grateful to my parents, my younger brother, my parents-in-law, and my sister-in-law for assuming some of the responsibilities of being a father during my time away from China.

Affidavit

Zhang, Hengliang

Surname, first name

I hereby declare, that the submitted thesis entitled

Retinoic acid modulation guides human-induced pluripotent stem cell differentiation towards left or right ventricle-like cardiomyocytes

is my own work. I have only used the sources indicated and have not made unauthorised use of services of a third party. Where the work of others has been quoted or reproduced, the source is always given.

I further declare that the dissertation presented here has not been submitted in the same or similar form to any other institution for the purpose of obtaining an academic degree.

Munich, 22.06.2024

Place, Date

Hengliang Zhang

Signature doctoral candidate